TJ dynamics

TJs are complexes of transmembrane and peripheral membrane proteins, including occludin, claudins, ZO-1 and ZO-2 [6]. The TJ structure is highly dynamic and undergoes continuous remodeling through unique kinetics [32]. The properties of TJs are determined by these dynamics [33].

Occludin S408 dephosphorylation reduces paracellular cation influx by stabilizing the occludin–ZO-1 interaction, leading to enhancement of claudin-1 and claudin-2 exchange and reduction of their pore formation at the TJ. By contrast, occludin S408 phosphorylation enhances homotypic occludin–occludin interactions, leading to the release of ZO-1 and formation of claudin-1- and claudin-2-based pores. Therefore, occludin S408 phosphorylation is a key factor in the remodeling of the claudin–occludin–ZO-1 interaction [34].

Claudin-1 is stably localized in TJs [35]. Most occludin is mobile and diffused within the junctional membrane. By contrast, most ZO-1 is continuously exchanged between the membrane and cytosol pools [34]. Fluorescence recovery after photo-bleaching (FRAP) analysis provided new insights into the dynamics of TJs. The perijunctional actomyosin ring contributes to myosin light chain kinase (MLCK)-dependent TJ regulation. FRAP analysis showed that TJ-associated ZO-1 exists in three pools: a fixed pool, a fast exchangeable pool associated with the cytosolic pool, and a slow exchangeable pool associated with the cytosolic pool. The exchange between the TJ pools and the cytosolic pool is regulated by MLCK [36]. Claudin dynamics differ depending on the particular claudin. Claudins forming TJ strands showed slower dynamics than those not forming TJ strands. Distinct claudin stabilities might affect how TJs regulate paracellular permeability by altering paracellular flux and paracellular ion permeability [37].

These insights into the dynamics of TJs address the molecular mechanism of paracellular homeostasis and will hopefully lead to the development of TJ-targeted tissue-specific and solute-specific drug delivery systems.

Epithelial barrier as the first line of defense against pathological microorganisms

The human mucosa has a surface area equivalent to 1.5 tennis courts. This large surface area means that there is significant risk of infection by pathological microorganisms; therefore, homeostasis of the epithelial barrier is important. Indeed, some pathogens modulate the epithelial barrier to facilitate easy and widespread infection (Fig. 2a).

Modulation of the epithelial barrier by pathogens

Human immunodeficiency virus-1 (HIV-1) infection is often associated with increased permeability of mucosal epithelial cells. Viral envelope glycoprotein (gp)120 is a crucial viral protein that increases the permeability of the epithelial barrier. When HIV-1 binds to cells it induces production of TNF-α, leading to a decrease in mucosal epithelial barrier integrity and spread of HIV-1 infection [38].

Atopic dermatitis (AD) is the most common inflammatory skin disease [39], and susceptibility to cutaneous infections is increased in AD patients. Widespread skin infection by the herpes simplex virus (HSV) causes severe viral complications, such as eczema herpeticum in AD patients. Defects in the epidermal TJ barrier increase the susceptibility of patients with AD to widespread subcutaneous infection with HSV or other viral pathogens [40]. In the early stage of infection with enterohemorrhagic *Escherichia coli* (EHEC), non-bloody diarrhea occurs in the absence of shiga toxin. EHEC infection increases expression of claudin-2 and redistribution of claudin-3 and occludin. These changes correlate with increased intestinal permeability [41]. Infection by enteroaggregative *Escherichia coli* (EAEC) causes dissociation of claudin-1 from the TJs between epithelial cells, leading to disruption of the TJ barrier [42]. By contrast, respiratory syncytial virus (RSV) increases TJ integrity. RSV is the major cause of bronchitis, asthma and severe lower respiratory tract diseases in infants and young children [43]. RSV infection induces expression of claudin-4 and occludin in human nasal epithelial cells. Induction of TJ components has a crucial role in epithelial cellular polarity, leading to budding of the virus from the epithelial apical surface [44]. Therefore, prevention of TJ barrier modulation by pathogens might be a viable therapeutic strategy.

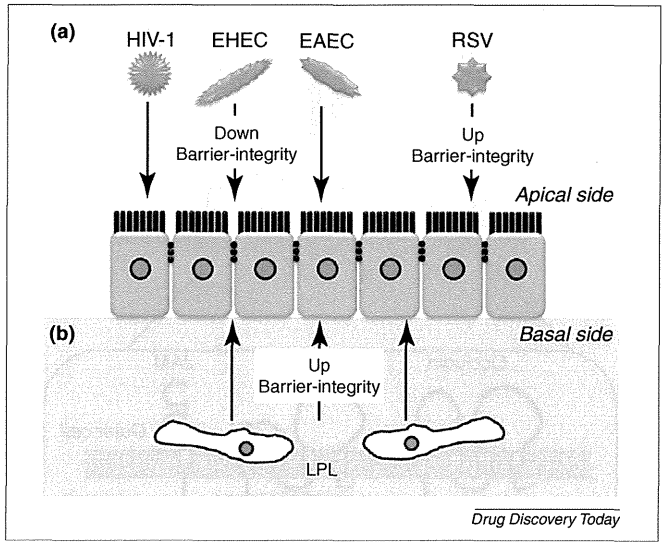

FIGURE 2

Regulation of the first line of defense, the epithelial barrier. **(a)** Pathological microorganism–epithelial barrier interaction. Infection of epithelial cells by HIV-1, EHEC, or EAEC decreased epithelial barrier integrity [38,41,42]. By contrast, RSV infection increased the barrier function [44]. **(b)** Lymphocyte–epithelial barrier interaction. LPLs regulate the integrity of the epithelial barrier via direct interaction with epithelial cells through notch signaling [49]. *Abbreviations*: EAEC: enteroaggregative *Escherichia coli*; EHEC: enterohemorrhagic *Escherichia coli*; HIV-1: human immunodeficiency virus-1; LPLs: lamina propria lymphocytes; RSV: respiratory syncytial virus.

Lymphoepithelial cross talk in the epithelial barrier

Mucosa-associated lymphoid tissues (MALTs) are lymphoid immune tissues that are located in the mucosal epithelium. By activating mucosal immune responses, they function as the first line of defense against pathogens invading the body through the epithelium [45]. MALTs comprise gut-associated lymphoid tissues, nasopharynx-associated lymphoid tissues and bronchus-associated lymphoid tissues. MALTs contain lymphocytes, M cells, T cells, B cells and antigen-presenting cells. Recently, lamina propria lymphocytes (LPLs) underlying the intestinal epithelium have

Please cite this article in press as: A. Takahashi, et al., Pathological changes in tight junctions and potential applications into therapies, Drug Discov Today (2012), doi:10.1016/j.drudis.2012.02.014

been shown to have a crucial role in the homeostasis of the epithelial barrier (Fig. 2b). Direct interaction of LPLs with intestinal epithelial cells is essential for the barrier function of the intestinal epithelium [46]. The notch signaling pathway regulates cell fate decisions through cell–cell interactions [47]. Notch signaling determines the differentiation of intestinal stem cells into secretory cells, absorptive cells, or enterocytes [47,48]. The absence of LPLs in mice causes increased intestinal permeability and a lack of activation of notch in colonocytes [49]. Transfer of LPLs to LPL-deficient mice decreased intestinal permeability and activated notch signaling in colonocytes. In Caco-2 cells, knockdown of notch mRNA reduced the epithelial barrier function, and was accompanied by upregulation of claudin-2 proteins, reduction of occludin and cytoplasmic localization of claudin-5 [49]. Therefore, lymphoepithelial cross talk might regulate epithelial differentiation and barrier integrity. Notch signaling is highly activated in the mucosa of patients with Crohn's disease, leading to dysregulation of the differentiation of epithelial cells [49]. Normalization of disruption of this cross talk might be a potent strategy for treating immune-mediated intestinal disorders.

Proof-of-concept for TJ-targeted drug development

As mentioned in the introduction, epithelial cells are a potent target for drug development. TJ-targeted drug development has been attempted [14,50], and proof-of-concepts for TJ-targeted drug absorption, cancer targeting and mucosal vaccination have been established. Recent findings indicate that TJ-targeted therapy for hepatitis C virus (HCV), diabetes and inflammatory diseases might be possible.

HCV infection

A total of 170 million people worldwide are infected with the HCV. Hepatitis C is the leading cause of chronic liver inflammation, cirrhosis and cancer. Claudin-1 and occludin are co-receptors for HCV infection, indicating that binders to claudin-1 or occludin might be potent inhibitors of HCV entry [16]. DNA immunization enabled successful preparation of monoclonal anti-claudin-1 antibodies against the extracellular loop of claudin-1, and these anti-claudin-1 antibodies prevented HCV infection. Antibodies effectively blocked cell entry of highly infectious escape variants of HCV that were resistant to neutralizing antibodies [51]. When hepatitis C patients reach end-stage liver failure, liver transplantation is the only choice for curative treatment; however, reinfection of the transplanted liver by HCV often occurs. There is a significant correlation between hepatic levels of claudin-1 and occludin and HCV reinfection after liver transplantation [52]. Inhibition of HCV reinfection of the transplanted liver by using anti-claudin-1 antibodies might be a potent treatment for patients with liver transplantation.

Diabetic retinopathy

Breakdown of the blood–retinal barrier (BRB) is a hallmark of diabetic retinopathy [53]. Alterations to the BRB occur early in the progression of diabetic retinopathy and eventually lead to macular edema, which is responsible for vision loss [54]. Diabetic patients show elevated levels of TNF-α in the vitreous humor. TNF-α increases the permeability of retinal endothelial cells. TNF-α decreases ZO-1 and claudin-5 expression and alters cellular localization of ZO-1 and claudin-5 [55]. Thus, regulation of BRB-integrity might be a potent strategy for treating vision loss owing to diabetes. Indeed, a chemical already in clinical use for the treatment of diabetic retinopathy, calcium dobesilate, attenuates the decrease in occludin and claudin-5 and prevents BRB breakdown [56]. Berberine, a plant alkaloid, has also been used for the treatment of diabetes. Berberine prevents barrier defects in retinal epithelial cells [57]. Inducers of occludin and claudin-5 or promoters of TJ integrity could be a potent treatment for diabetic retinopathy.

Inflammatory diseases

Berberine has been also used in the treatment of gastroenteritis and diarrhea. TNF-α disrupts TJ integrity in inflammatory bowel diseases (IBD). Regulation of the TNF-α-dependent signaling pathway is a potent strategy for the treatment of IBD. TNF-α removes claudin-1 from TJs and induces claudin-2 expression, leading to disruption of the TJ barrier. Attenuation of TNF-α signaling is a potent strategy for IBD therapy. Berberine also attenuates TNF-α-induced TJ barrier defects by removing claudin-1 and inducing claudin-2 expression [58]. Spontaneous colitis was observed in interleukin (IL)-10−/− mice in which paracellular permeability was increased in conjunction with decreased expression and redistribution of ZO-1, occludin and claudin-1. Treatment with a probiotic, *Lactobacillus plantarum*, restored expression of TJ components and TJ integrity, resulting in prevention of bacterial translocation and proinflammatory responses in IL-10−/− mice [59]. Recovery of TJ integrity might be a potent strategy for inflammatory intestinal diseases. Ouabain, which is an inhibitor of Na^+, K^+-ATPase, increased TJ integrity through signaling pathways involving c-Src and ERK1/2 and by modulating the expression of claudin-1, claudin-2 and claudin-4 [60,61]. Several natural products have been found to be therapeutically useful against epithelial barrier defects.

Paracellular drug transport

The claudin protein family comprises 27 members [7]. Claudins form homo- and hetero-type strands in the lateral membrane. Adjacent claudin-based TJ strands associate with each other, leading to sealing of the intercellular space. The combination of the claudin members is a determinant factor for the properties of the TJ barrier [5]. These findings suggest that optimization of claudin modulators with narrow-specificity in certain cases, or broad-specificity in other cases, might regulate solute- and tissue-specificity in paracellular transport. The most important issue in TJ-targeted drug absorption is the development of claudin modulators. Claudin is an integral membrane protein with a tetra-transmembrane domain. Claudin binders are the first choice for claudin modulators. The first extracellular loop contains approximately 50 amino acids and the second contains approximately ten amino acids. Claudins are hydrophobic proteins, and preparation of a recombinant protein is only currently possible for claudin-4 [62]. Therefore, the development of claudin binders, including antibodies, has been slow. Budded baculoviruses display functional forms of membrane proteins on their surface [63]. Claudin-displaying budded baculoviruses possess a native form of claudin and can be used as a screening system for claudin binders [64]. Functional membrane proteins are heterogeneously expressed on

Please cite this article in press as: A. Takahashi, et al., Pathological changes in tight junctions and potential applications into therapies, Drug Discov Today (2012), doi:10.1016/j.drudis.2012.02.014

budded baculoviruses [63]. Functional information using FRAP analysis will enable development of a screening system for claudin modulators with narrow- or broad-specificity using the heterogenous claudin-displaying baculoviral system. We predict that, in the near future, proof-of-concept for tissue- and solute-specific paracellular transport by modulating the claudin-barrier will be demonstrated.

Coupling of transcellular and paracellular transport systems controls permeability to solutes [65]. Claudin-based TJs function as charge-selective paracellular channels [6]. Claudin-15 is responsible for transepithelial permeability to extracellular monovalent cations, especially Na^+. Claudin-15-deficient mice exhibit low luminal Na^+ levels and low glucose absorption in the intestine, indicating that paracellular transport of Na^+ through claudin-15-based TJ strands might be coupled to transcellular transport of glucose through a glucose transporter [66]. These findings suggest that modulation of the claudin-mediated paracellular transport of solutes might regulate the transcellular transport of drugs through a transporter.

Concluding remarks

To our knowledge, the first report of TJ-targeted drug development was the discovery in 1961 of enhanced mucosal absorption of drugs by co-administration of ethylenediaminetetraacetic acid [67]. TJs were identified in 1963 [17]. Modulation of the TJ-barrier has been a major strategy for enhancing mucosal absorption; however, the biochemical structure of TJs was unclear until 1998. Until that year, absorption enhancers were screened mainly by modulating epithelial cell sheets. Recent imaging studies have begun to reveal the dynamics of TJs and also how these dynamics are regulated [36,37]. Future detailed analyses using FRAP will provide us with new insights into strategies for modulation of the TJ barrier. In addition to TJ-modulated drug absorption, TJ-targeted therapy for HCV infection and diabetic retinopathy has recently been proved effective [51,56]. The questions of how TJ dynamics are regulated, and how expression of TJ components is regulated are still to be answered. The molecular pathology of deregulation of the TJ barrier is not yet fully understood. TJ-targeted drug development has been spearheaded by rapid progress in our understanding of the biology of the TJ barrier.

Acknowledgements

This work was supported in part by a Grant-in-Aid for Scientific Research from the Ministry of Education, Culture, Sports, Science and Technology, Japan (21689006) and by Health and Labor Sciences Research Grants from the Ministry of Health, Labor and Welfare of Japan. AT and HS are supported by Research Fellowships of the Japan Society for the Promotion of Science for Young Scientists.

References

1 Anderson, J.M. and Van Itallie, C.M. (1995) Tight junctions and the molecular basis for regulation of paracellular permeability. *Am. J. Physiol.* 269 (4 Pt 1), G467–G475
2 Gumbiner, B. (1993) Breaking through the tight junction barrier. *J. Cell Biol.* 123, 1631–1633
3 Staehelin, L.A. (1973) Further observations on the fine structure of freeze-cleaved tight junctions. *J. Cell Sci.* 13, 763–786
4 Chiba, H. *et al.* (2008) Transmembrane proteins of tight junctions. *Biochim. Biophys. Acta* 1778, 588–600
5 Furuse, M. and Tsukita, S. (2006) Claudins in occluding junctions of humans and flies. *Trends Cell Biol.* 16, 181–188
6 Van Itallie, C.M. and Anderson, J.M. (2009) Physiology and function of the tight junction. *Cold Spring Harb. Perspect. Biol.* 1, a002584
7 Mineta, K. *et al.* (2011) Predicted expansion of the claudin multigene family. *FEBS Lett.* 585, 606–612
8 Ikenouchi, J. *et al.* (2005) Tricellulin constitutes a novel barrier at tricellular contacts of epithelial cells. *J. Cell Biol.* 171, 939–945
9 Sanchez-Pulido, L. *et al.* (2002) MARVEL: a conserved domain involved in membrane apposition events. *Trends Biochem. Sci.* 27, 599–601
10 Raleigh, D.R. *et al.* (2010) Tight junction-associated MARVEL proteins marvelD3, tricellulin, and occludin have distinct but overlapping functions. *Mol. Biol. Cell* 21, 1200–1213
11 Umeda, K. *et al.* (2006) ZO-1 and ZO-2 independently determine where claudins are polymerized in tight-junction strand formation. *Cell* 126, 741–754
12 Masuda, S. *et al.* (2011) LSR defines cell corners for tricellular tight junction formation in epithelial cells. *J. Cell Sci.* 124 (Pt 4), 548–555
13 Furuse, M. (2010) Molecular basis of the core structure of tight junctions. *Cold Spring Harb. Perspect. Biol.* 2, a002907
14 Takahashi, A. *et al.* (2011) Claudin as a target for drug development. *Curr. Med. Chem.* 18, 1861–1865
15 Turksen, K. and Troy, T.C. (2011) Junctions gone bad: claudins and loss of the barrier in cancer. *Biochim. Biophys. Acta* 1816, 73–79
16 Zeisel, M.B. *et al.* (2011) Hepatitis C virus entry into hepatocytes: molecular mechanisms and targets for antiviral therapies. *J. Hepatol.* 54, 566–576
17 Farquhar, M.G. and Palade, G.E. (1963) Junctional complexes in various epithelia. *J. Cell Biol.* 17, 375–412
18 Nusrat, A. *et al.* (2000) Molecular physiology and pathophysiology of tight junctions. IV. Regulation of tight junctions by extracellular stimuli: nutrients, cytokines, and immune cells. *Am. J. Physiol.* 279, G851–G857
19 Furuse, M. *et al.* (1993) Occludin: a novel integral membrane protein localizing at tight junctions. *J. Cell Biol.* 123 (6 Pt 2), 1777–1788
20 Saitou, M. *et al.* (1998) Occludin-deficient embryonic stem cells can differentiate into polarized epithelial cells bearing tight junctions. *J. Cell Biol.* 141, 397–408
21 Furuse, M. *et al.* (1998) A single gene product, claudin-1 or -2, reconstitutes tight junction strands and recruits occludin in fibroblasts. *J. Cell Biol.* 143, 391–401
22 Furuse, M. (2009) Knockout animals and natural mutations as experimental and diagnostic tool for studying tight junction functions *in vivo*. *Biochim. Biphys. Acta* 1788, 813–819
23 Stevenson, B.R. *et al.* (1986) Identification of ZO-1: a high molecular weight polypeptide associated with the tight junction (zonula occludens) in a variety of epithelia. *J. Cell Biol.* 103, 755–766
24 Staehelin, L.A. *et al.* (1969) Freeze-etch appearance of the tight junctions in the epithelium of small and large intestine of mice. *Protoplasma* 67, 165–184
25 Friend, D.S. *et al.* (1972) Variations in tight and gap junctions in mammalian tissues. *J. Cell Biol.* 53, 375–412
26 Ikenouchi, J. *et al.* (2008) Loss of occludin affects tricellular localization of tricellulin. *Mol. Biol. Cell* 19, 4687–4693
27 Lin, J.E. *et al.* (2009) Guanylyl cyclase C in colorectal cancer: susceptibility gene and potential therapeutic target. *Future Oncol.* 5, 509–522
28 Lorenz, J.N. *et al.* (2003) Uroguanylin knockout mice have increased blood pressure and impaired natriuretic response to enteral NaCl load. *J. Clin. Invest.* 112, 1244–1254
29 Han, X. *et al.* (2011) Loss of guanylyl cyclase C (GCC) signaling leads to dysfunctional intestinal barrier. *PLoS ONE* 6, E16139
30 Bugge, T.H. *et al.* (2007) Matriptase-dependent cell surface proteolysis in epithelial development and pathogenesis. *Front. Biosci.* 12, 5060–5070
31 Buzza, M.S. *et al.* (2010) Membrane-anchored serine protease matriptase regulates epithelial barrier formation and permeability in the intestine. *Proc. Natl. Acad. Sci. U. S. A.* 107, 4200–4205
32 Ikenouchi, J. *et al.* (2003) Regulation of tight junctions during the epithelium–mesenchyme transition: direct repression of the gene expression of claudins/occludin by Snail. *J. Cell Sci.* 116 (Pt 10), 1959–1967
33 Steed, E. *et al.* (2010) Dynamics and functions of tight junctions. *Trends Cell Biol.* 20, 142–149
34 Raleigh, D.R. *et al.* (2011) Occludin S408 phosphorylation regulates tight junction protein interactions and barrier function. *J. Cell Biol.* 193, 565–582

Please cite this article in press as: A. Takahashi, et al., Pathological changes in tight junctions and potential applications into therapies, Drug Discov Today (2012), doi:10.1016/j.drudis.2012.02.014

35 Sasaki, H. *et al.* (2003) Dynamic behavior of paired claudin strands within apposing plasma membranes. *Proc. Natl. Acad. Sci. U. S. A.* 100, 3971–3976
36 Yu, D. *et al.* (2010) MLCK-dependent exchange and actin binding region-dependent anchoring of ZO-1 regulate tight junction barrier function. *Proc. Natl. Acad. Sci. U. S. A.* 107, 8237–8241
37 Yamazaki, Y. *et al.* (2011) Role of claudin species-specific dynamics in reconstitution and remodeling of the zonula occludens. *Mol. Biol. Cell* 22, 1495–1504
38 Nazli, A. *et al.* (2010) Exposure to HIV-1 directly impairs mucosal epithelial barrier integrity allowing microbial translocation. *PLoS Pathog.* 6, E1000852
39 Beck, L.A. *et al.* (2009) Phenotype of atopic dermatitis subjects with a history of eczema herpeticum. *J. Allergy Clin. Immunol.* 124, 260–269 269 E261–E267
40 De Benedetto, A. *et al.* (2011) Reductions in claudin-1 may enhance susceptibility to herpes simplex virus 1 infections in atopic dermatitis. *J. Allergy Clin. Immunol.* 128, 242–246 E245
41 Roxas, J.L. *et al.* (2010) Enterohemorrhagic *E. coli* alters murine intestinal epithelial tight junction protein expression and barrier function in a Shiga toxin independent manner. *Lab. Invest.* 90, 1152–1168
42 Strauman, M.C. *et al.* (2010) Enteroaggregative *Escherichia coli* disrupts epithelial cell tight junctions. *Infect. Immun.* 78, 4958–4964
43 Bitko, V. and Barik, S. (1998) Persistent activation of RelA by respiratory syncytial virus involves protein kinase C, underphosphorylated IkappaBbeta, and sequestration of protein phosphatase 2A by the viral phosphoprotein. *J. Virol.* 72, 5610–5618
44 Masaki, T. *et al.* (2011) A nuclear factor-kappaB signaling pathway via protein kinase C delta regulates replication of respiratory syncytial virus in polarized normal human nasal epithelial cells. *Mol. Biol. Cell* 22, 2144–2156
45 Kunisawa, J. *et al.* (2008) Immunological commonalities and distinctions between airway and digestive immunity. *Trends Immunol.* 29, 505–513
46 Dahan, S. *et al.* (2009) Lymphoepithelial interactions: a new paradigm. *Ann. N. Y. Acad. Sci.* 1165, 323–326
47 Kopan, R. and Ilagan, M.X. (2009) The canonical Notch signaling pathway: unfolding the activation mechanism. *Cell* 137, 216–233
48 Hermiston, M.L. *et al.* (1993) Chimeric-transgenic mice represent a powerful tool for studying how the proliferation and differentiation programs of intestinal epithelial cell lineages are regulated. *Proc. Natl. Acad. Sci. U. S. A.* 90, 8866–8870
49 Dahan, S. *et al.* (2011) Notch-1 signaling regulates intestinal epithelial barrier function, through interaction with $CD4^+$ T cells, in mice and humans. *Gastroenterology* 140, 550–559
50 Kondoh, M. *et al.* (2008) Targeting tight junction proteins – significance for drug development. *Drug Discov. Today* 13, 180–186
51 Fofana, I. *et al.* (2010) Monoclonal anti-claudin 1 antibodies prevent hepatitis C virus infection of primary human hepatocytes. *Gastroenterology* 139, 953–964 964 E951–E954
52 Mensa, L. *et al.* (2011) Hepatitis C virus receptors claudin-1 and occludin after liver transplantation and influence on early viral kinetics. *Hepatology* 53, 1436–1445
53 Cunha-Vaz, J. *et al.* (1975) Early breakdown of the blood–retinal barrier in diabetes. *Br. J. Ophthalmol.* 59, 649–656
54 The Diabetes Control and Complications Trial Research Group, (1993) The effect of intensive treatment of diabetes on the development and progression of long-term complications in insulin-dependent diabetes mellitus. *N. Engl. J. Med.* 329, 977–986
55 Aveleira, C.A. *et al.* (2010) TNF-alpha signals through PKCzeta/NF-kappaB to alter the tight junction complex and increase retinal endothelial cell permeability. *Diabetes* 59, 2872–2882
56 Leal, E.C. *et al.* (2010) Calcium dobesilate inhibits the alterations in tight junction proteins and leukocyte adhesion to retinal endothelial cells induced by diabetes. *Diabetes* 59, 2637–2645
57 Cui, H.S. *et al.* (2007) Effect of berberine on barrier function in a human retinal pigment epithelial cell line. *Jpn. J. Ophthalmol.* 51, 64–67
58 Amasheh, M. *et al.* (2010) TNFalpha-induced and berberine-antagonized tight junction barrier impairment via tyrosine kinase, Akt and NFkappaB signaling. *J. Cell Sci.* 123 (Pt 23), 4145–4155
59 Chen, H.Q. *et al.* (2010) Lactobacillus plantarum ameliorates colonic epithelial barrier dysfunction by modulating the apical junctional complex and PepT1 in IL-10 knockout mice. *Am. J. Physiol.* 299, G1287–G1297
60 Larre, I. *et al.* (2010) Ouabain modulates epithelial cell tight junction. *Proc. Natl. Acad. Sci. U. S. A.* 107, 11387–11392
61 Larre, I. *et al.* Ouabain modulates ciliogenesis in epithelial cells. *Proc. Natl. Acad. Sci. U. S. A.*, doi:10.1073/pnas.1102617108 (in press)
62 Mitic, L.L. *et al.* (2003) Expression, solubilization, and biochemical characterization of the tight junction transmembrane protein claudin-4. *Protein Sci.* 12, 218–227
63 Sakihama, T. *et al.* (2008) Functional reconstitution of G-protein-coupled receptor-mediated adenylyl cyclase activation by a baculoviral co-display system. *J. Biotechnol.* 135, 28–33
64 Kakutani, H. *et al.* (2011) A novel screening system for claudin binder using baculoviral display. *PLoS ONE* 6, E16611
65 Kapus, A. and Szaszi, K. (2006) Coupling between apical and paracellular transport processes. *Biochem. Cell Biol.* 84, 870–880
66 Tamura, A. *et al.* (2011) Loss of claudin-15, but not claudin-2, causes Na(+) deficiency and glucose malabsorption in mouse small intestine. *Gastroenterology* 140, 913–923
67 Windsor, E. and Cronheim, G.E. (1961) Gastro-intestinal absorption of heparin and synthetic heparinoids. *Nature* 190, 263–264
68 Gonzalez-Mariscal, L. *et al.* (2000) MAGUK proteins: structure and role in the tight junction. *Semin. Cell Dev. Biol.* 11, 315–324

Please cite this article in press as: A. Takahashi, et al., Pathological changes in tight junctions and potential applications into therapies, Drug Discov Today (2012), doi:10.1016/j.drudis.2012.02.014

Biochemical and Biophysical Research Communications 426 (2012) 454–460

Contents lists available at SciVerse ScienceDirect

Biochemical and Biophysical Research Communications

journal homepage: www.elsevier.com/locate/ybbrc

A simple reporter assay for screening claudin-4 modulators

Akihiro Watari, Kiyohito Yagi, Masuo Kondoh *

Laboratory of Bio-Functional Molecular Chemistry, Graduate School of Pharmaceutical Sciences, Osaka University, Suita, Osaka 565-0871, Japan

ARTICLE INFO

Article history:
Received 15 August 2012
Available online 27 August 2012

Keywords:
Claudin
Tight junction
Reporter assay
Screening
Chemical modulator

ABSTRACT

Claudin-4, a member of a tetra-transmembrane protein family that comprises 27 members, is a key functional and structural component of the tight junction-seal in mucosal epithelium. Modulation of the claudin-4-barrier for drug absorption is now of research interest. Disruption of the claudin-4-seal occurs during inflammation. Therefore, claudin-4 modulators (repressors and inducers) are promising candidates for drug development. However, claudin-4 modulators have never been fully developed. Here, we attempted to design a screening system for claudin-4 modulators by using a reporter assay. We prepared a plasmid vector coding a claudin-4 promoter-driven luciferase gene and established stable reporter gene-expressing cells. We identified thiabendazole, carotene and curcumin as claudin-4 inducers, and potassium carbonate as a claudin-4 repressor by using the reporter cells. They also increased or decreased, respectively, the integrity of the tight junction-seal in Caco-2 cells. This simple reporter system will be a powerful tool for the development of claudin-4 modulators.

1. Introduction

Tight junctions (TJs), the most apical components of intercellular junctional complexes, function as fences that maintain cellular polarity and provide a barrier to regulate intercellular permeability of epithelia [1,2]. Disruption of cellular polarity and the TJ-seal is frequently observed during carcinogenesis and inflammation [3]. Modulation of TJ-seals for drug absorption is now of research interest [4,5]. A series of studies has revealed that TJs are composed of transmembrane proteins (such as occludin and claudins), junction adhesion proteins, and cytoplasmic scaffolding proteins, including ZO-1, ZO-2, and ZO-3 (see reviews [6–8]). Of these, claudins are thought to be the main structural and functional components of TJs.

Claudins, tetra-transmembrane proteins with a molecular mass of approximately 23 kDa, comprise a multigene family containing over 20 members [8]. The barrier-function and the expression patterns of claudin members differ among tissues [6,8,9]. Claudin-1-, -5-, and -11-deficient mice show dysfunction of the epidermal barrier, blood–brain barrier, and blood–testis barrier, respectively [10–12]. The expression levels and the barrier-functions of claudins are often altered in various cancer cells; they can be down-regulated or up-regulated, depending on the type of cancer [13]. Changes in claudin expression have also been observed in the mucosal epithelium under inflammatory conditions [14]. Claudins are thus potent targets for drug development, such as drug delivery, anti-cancer agents, and anti-inflammatory agents.

Since claudins play a role in TJ-seals, modulation of the claudin-barrier is a potent strategy for drug absorption. The carboxyl-terminus of *Clostridium perfringens* enterotoxin (C-CPE) is a modulator of the claudin-barrier [15]. Treatment of cells with C-CPE causes a decrease in claudin-4 proteins in TJs, followed by an enhancement of the paracellular transport of solutes without causing cytotoxicity [15]. C-CPE also enhances jejunal, nasal, and pulmonary absorption of drugs [16]. Thus, proof-of-concept for claudin-targeted drug absorption has been demonstrated. A decrease in claudin-4 in the intestinal epithelium often occurs in colitis [17]. Down-regulation of claudin-4 is also observed in some cancer cells [18]. Induction of claudin-4 is involved in the chemo-preventive effect of nonsteroidal anti-inflammatory drugs [19]. A modulator of claudin-4 expression would therefore be a potent molecule for claudin-targeted drug absorption and drug development for some inflammatory diseases and cancers. However, an effective system to screen for claudin modulators is lacking.

Here, we developed a simple system to monitor claudin-4 expression using a reporter gene, and we screened chemical claudin-4 modulators.

Abbreviations: TJs, tight junctions; C-CPE, the carboxyl terminus of *Clostridium perfringens* enterotoxin; TGF-β, transforming growth factor-β; EGF, epidermal growth factor; PMA, phorbol 12-myristate 13-acetate; DMSO, dimethyl sulfoxide; PCR, polymerase chain reaction; RT-PCR, reverse transcription-PCR; GAPDH, glyceraldehyde 3-phosphate dehydrogenase; qPCR, quantitative PCR; SDS, sodium dodecyl sulfate; SDS-PAGE, SDS-polyacrylamide gel electrophoresis; TER, transepithelial electric resistance.

* Corresponding author. Fax: +81 6 6879 8199.
E-mail address: masuo@phs.osaka-u.ac.jp (M. Kondoh).

0006-291X/$ - see front matter © 2012 Elsevier Inc. All rights reserved.
http://dx.doi.org/10.1016/j.bbrc.2012.08.083

2. Materials and methods

2.1. Reagents and cells

Recombinant human transforming growth factor-β (TGF-β) and epidermal growth factor (EGF) were purchased from R&D systems (Minneapolis, MN) and Peprotech Inc. (Rocky Hill, NJ), respectively. The recombinant proteins were dissolved in water and stored at −80 °C before use. Phorbol 12-myristate 13-acetate (PMA) were dissolved in dimethyl sulfoxide (DMSO) and stored at −20 °C before use. List of the chemicals used in this study for screening for claudin-4 modulator is shown in Table 1. All reagents were of research grade.

MCF-7, and Caco-2 cells were cultured in Dulbecco's modified minimal essential medium supplemented with 10% fetal bovine serum in 5% CO_2 at 37 °C. MCF-7 cells were obtained from the RIKEN cell bank (Ibaragi, Japan). Caco-2 cells were obtained from the American Type Culture Collection (Manassas, VA). MCF-7 cells stably expressing snail or HRasV12 were prepared by infection with a recombinant retroviral vector coding for snail or HRasV12 gene.

2.2. Preparation of a reporter plasmid

Genomic DNA was extracted from MCF-7 cells by using a genomic DNA isolation kit (Sigma–Aldrich, St. Louis, MO). The claudin-4 promoter region was cloned by polymerase chain reaction (PCR) using genomic DNA as a template and paired primers (forward primer, 5′-GCGCTAGCGGTTGCCCCCTGGCCTTAAC-3′; reverse primer, 5′-CGCTCGAGGTCCACGGGAGTTGAGGACC-3′). The resultant fragments (500 bp) were subcloned into the pGV-B2 vector encoding the luciferase gene (Toyobo, Osaka, Japan). The sequence of the claudin-4 promoter region was confirmed.

2.3. A transient expression of transfection snail or HRasV12 gene

Transfection was performed with FuGENE HD (Roche, Mannheim, Germany) according to the manufacturer's protocol. Briefly, cells were seeded onto 24-well plates. When the cells reached to 80% confluent cell density, 20 μl of medium containing 0.6 μl of FuGENE HD and 200 ng of plasmid carrying snail or HRasV12 gene was added to the wells. After 48 h of transfection, the luciferase activity of the cell lysates was measured as described below.

2.4. Luciferase assay

Luciferase activity was measured using a commercial available luciferase assay system (Toyo Ink, Tokyo, Japan). Cells were lysed with a cell lysis reagent, LCβ (Toyo Ink). The cell lysates were then centrifuged at *18,000g* for 5 min. The luciferase activity in the resulting supernatant was measured using a TriStar LB 941 microplate reader (Berthold, Wildbad, Germany).

2.5. Establishment of a stable reporter cell line

MCF-7 cells were transfected with the reporter plasmid and a plasmid carrying the puromycin resistance gene. Stable transfectants were selected in the presence of puromycin.

2.6. Screening for claudin-4 modulators

The clone 35 cells were seeded onto 96-well plates at a density of 4×10^4 cells/well. On the following day, vehicle or compound was added, and the cells were cultured for an additional 24 h. The luciferase activity in the cells was then measured as described above.

2.7. Cytotoxicity assay

Clone 35 cells or Caco-2 cells were seeded onto a 96-well plate at a density of 4×10^4 or 6×10^4 cells/well, respectively. On the following day, cells were treated with chemicals at the indicated periods. The cell viability was measured by using a WST-8 assay kit (Nacalai, Kyoto, Japan).

2.8. Reverse transcription–PCR (RT–PCR) analysis

RT reaction and PCR amplification were performed with a cDNA synthesis kit (Roche, Mannheim, Germany) and ExTaqTM (Takara, Shiga, Japan), respectively, according to the manufacturer's instructions. Briefly, total RNA was prepared with TRIzol reagent (Invitrogen, Carlsbad, CA). For reverse transcription, 5 μg of total RNA was used. PCR was performed for 23 cycles for claudin-4 (94 °C for 30 s, 55 °C for 15 s, 72 °C for 30 s) and for 20 cycles for GADPH (94 °C for 30 s, 55 °C for 15 s, 72 °C for 60 s). The PCR products were separated by use of agarose gel electrophoresis and stained with ethidium bromide. The sequences of the primers are as follows: forward primer for claudin-4, 5′-CAACATTGTCACCTCGCAGACCATC-3′; reverse primer for claudin-4, 5′-TATCACCATAAGGCCGGCCAACAG-3′; forward primer for glyceraldehyde 3-phosphate dehydrogenase (GAPDH), 5′-TCTTCACCACCATGGAGAAG-3′; reverse primer for GAPDH, 5′-ACCACCTGGTGCTCAGTGTA-3′.

2.9. Quantitative PCR (qPCR) analysis

qPCR was performed with SYBR Premix Ex Taq II (Takara) using an Applied Biosystems StepOne Plus (Applied Biosystems, Foster City, CA). Relative quantification was performed against a standard curve and the values were normalized against the input determined for the housekeeping gene, GAPDH. The primer sequences used for qPCR were as follows: forward primer for claudin-4, 5′-TTGTCACCTCGCAGACCATC-3′ and reverse primer for claudin-4, 5′-CAGCGAGTCGTACACCTTG-3′; forward primer for GAPDH, 5′-GGTGGTCTCCTCTGACTTCAACA-3′ and reverse primer for GAPDH, 5′-GTGGTCGTTGAGGGCAATG-3′.

2.10. Western blot analysis

Cells were lysed with RIPA buffer (0.15 M NaCl, 50 mM Tris–HCl, pH 7.4, 1 mM ethylenediaminetetraacetic acid, 1% Triton X-100, 1% sodium deoxycholate, 0.1% sodium dodecyl sulfate (SDS), 1% protease inhibitor cocktail [Sigma–Aldrich]). The cell lysates were subjected to 15% SDS–polyacrylamide gel electrophoresis (SDS–PAGE), followed by blotting onto polyvinylidene difluoride membrane. The membranes were incubated with anti-claudin-4 mouse monoclonal (Zymed, South San Francisco, CA) and anti-β-actin mouse monoclonal (Sigma–Aldrich) antibodies, respectively, and subsequently treated with horseradish peroxidase-conjugated anti-mouse IgG (Zymed). The reactive bands were detected by using an enhanced chemiluminescence reagent (GE Healthcare, Buckinghamshire, UK).

2.11. Transepithelial electric resistance (TER) assay

Caco-2 cells were seeded into Transwell™ chambers (Corning, NY) at a density of 8×10^4 cells/well. On 7 days after the seeding or when TER values reached a plateau, claudin-4 inducers (thiabendazole, carotene, or curcumin) or claudin-4 repressor (potassium carbonate), respectively, was added. The TER values were then monitored at 0, 24, and 48 h using a Millicell-ERS epithelial

Table 1
Chemicals used in this study as screening sources.

Sample number	Sample name	Concentration[a]	Relative luciferase activity[b]
1	Tartrazine	10 mM	1.29
2	Potassium nitrate	1 mM	0.94
3	Potassium carbonate	10 mM	0.56
4	Sodium chlorous	10 mM	0.95
5	Zinc sulfate	0.1 mM	0.95
6	New coccine	0.01 mM	0.98
7	Amaranth (Bordeaux S)	1 mM	1.34
8	Allura red AC	1 mM	1.49
9	Sunset yellow FCF	1 mM	1.59
10	Potassium hydroxide	1 mM	0.83
11	L-ascorbic acid	1 mM	1.02
12	Sodium nitrite	10 mM	0.91
13	Propionic acid	0.0001%	0.82
14	Sodium carbonate	1 mM	0.91
15	Zinc gluconate	0.01%	1.76
16	Benzoic acid	0.01 mM	1.3
17	Sorbic acid	1 mM	1.51
18	Aspartame	1 mM	1.59
19	Dibutylhydroxytoluene	0.01 mM	1.81
20	Allyl isothiocyanate	0.0001%	1.72
21	Saccharin	1 mM	1.5
22	L-Ascorbyl palmitate	1 mM	1.21
23	Hydroxy biphenyl	0.01 mM	1.87
24	Aluminium potassium sulfate	0.1 mM	0.94
25	L-Lysine	10 mM	1.42
26	Calcium pantothenate	10 mM	1.61
27	Carrageenin	0.01 mM	1.56
28	Tartaric acid	1 mM	1.01
29	Sodium acetate	10 mM	1.02
30	Glycine	10 mM	1.68
31	Sodium alginate	10 mM	1.52
32	Ammonium chloride	10 mM	1.91
33	Magnesium sulfate	10 mM	1.56
34	5-Ribonucleotide	0.001 mM	1.15
35	Calcium chloride	1 mM	1.62
36	Valine	10 mM	1.08
37	Erythrosine	0.01 mM	1.22
38	Annatto	0.01 mM	1.96
39	Maltitol	10 mM	1.44
40	Sodium dehydroacetate	1 mM	1.98
41	Nicotinic acid	1 mM	1.55
42	Isoleucine	1 mM	1.06
43	Mannitol	10 mM	1.29
44	Ascorbic acid (Vitamin C)	10 mM	1.17
45	Phenylalanine	1 mM	0.95
46	Gallic acid	0.1 mM	1.41
47	Erythorbic acid (Sodium isoascorbate)	1 mM	1.03
48	Magnesium chloride	0.1%	1.26
49	Cochineal extract	0.1%	1.02
50	Calcium dihydrogen pyrophosphate	1 mM	1.1
51	Calcium citrate	0.01 mM	0.92
52	Polyvinyl acetate	0.1 mM	1.13
53	Fumaric acid	0.01 mM	1.24
54	Sodium methyl *p*-hydroxybenzoate	1 mM	2.04
55	Tocophenol (Vitamin E)	0.0001%	2.14
56	Rennet	0.01%	0.89
57	Ionone	0.01%	1.15
58	Isoeugenol	0.001%	1.15
59	Allyl isosulfocyanate	0.001%	1.06
60	Propylene glycol	0.1%	0.87
61	Ethyl isovalerate	0.001%	0.89
62	Pectin	0.001%	0.98
63	Cysteine	0.01 mM	0.76
64	Tragacanth gum	0.01%	0.83
65	Thiamin	0.1%	1.15
66	Gum arabic	0.01%	0.91
67	Cellulose	0.001%	0.84
68	Thiabendazole	0.1 mM	3.24
69	Isopropyl citrate	10 mM	1.04
70	γ-oryzanol	0.01%	1.02
71	Calcium carbonate	0.001%	0.857
72	Propylene glycol alginate	0.01%	0.87
73	Chlorophyll	0.1%	1.02
74	Sodium chondroitin sulfate	0.1%	1.04

Table 1 (*continued*)

Sample number	Sample name	Concentration[a]	Relative luciferase activity[b]
75	Biphenyl	0.1 mM	0.99
76	Sodium cytidylic acid	1 mM	0.77
77	Stevia rebaudiana	0.01%	0.96
78	Calcium stearoyl lactylate	0.01%	0.83
79	Ferrous sulfate	0.1 mM	1.37
80	Calcium sulfate	0.1 mM	0.93
81	Benzoyl peroxide	0.1 mM	1.13
82	Dibenzoyl thiamine	1 mM	0.88
83	Carotene	0.1 mM	2.09
84	Guar gum	0.001%	0.84
85	Xanthan gum	0.001%	0.77
86	Curcumin	0.01 mM	2.0

[a] The chemical concentrations were set at the maximum level to show no cytotoxicity.
[b] The relative luciferase activities were calculated as the ratio of that in the chemical-treated cells to that in the vehicle-treated cells. The treatment period was 24 h.

volt-ohmmeter (Millipore Corporation, Billerica, MA). The TER values were normalized to the area of the Caco-2 cell monolayers, and the TER value of a blank chamber was subtracted.

3. Results

3.1. Preparation of a reporter plasmid encoding a claudin-4-promoter-driven luciferase gene

As a first step toward developing a simple screening system for claudin-4 modulators, we cloned the promoter region of claudin-4. We searched for a region that was highly conserved among animals by using a UCSC Genome Bioinformatics program and cloned a 500 bp fragment corresponding to −293 to +194 bp of the claudin-4 gene. This 500 bp fragment contained various transcription factor-binding sites: an E-box (−276 to −271, −262 to −257, −221 to −216, −19 to −14, +10 to +14), a smad-binding element (SBE; −212 to −209, −103 to −100, −38 to −35), and Sp1 (−66 to −57, −53 to −44) [20,21], indicating that this region is a potent candidate for a regulatory region of claudin-4 expression. We constructed a reporter expression vector, in which the 500 bp fragment was inserted upstream of a luciferase gene Suppl. Fig. 1A). To

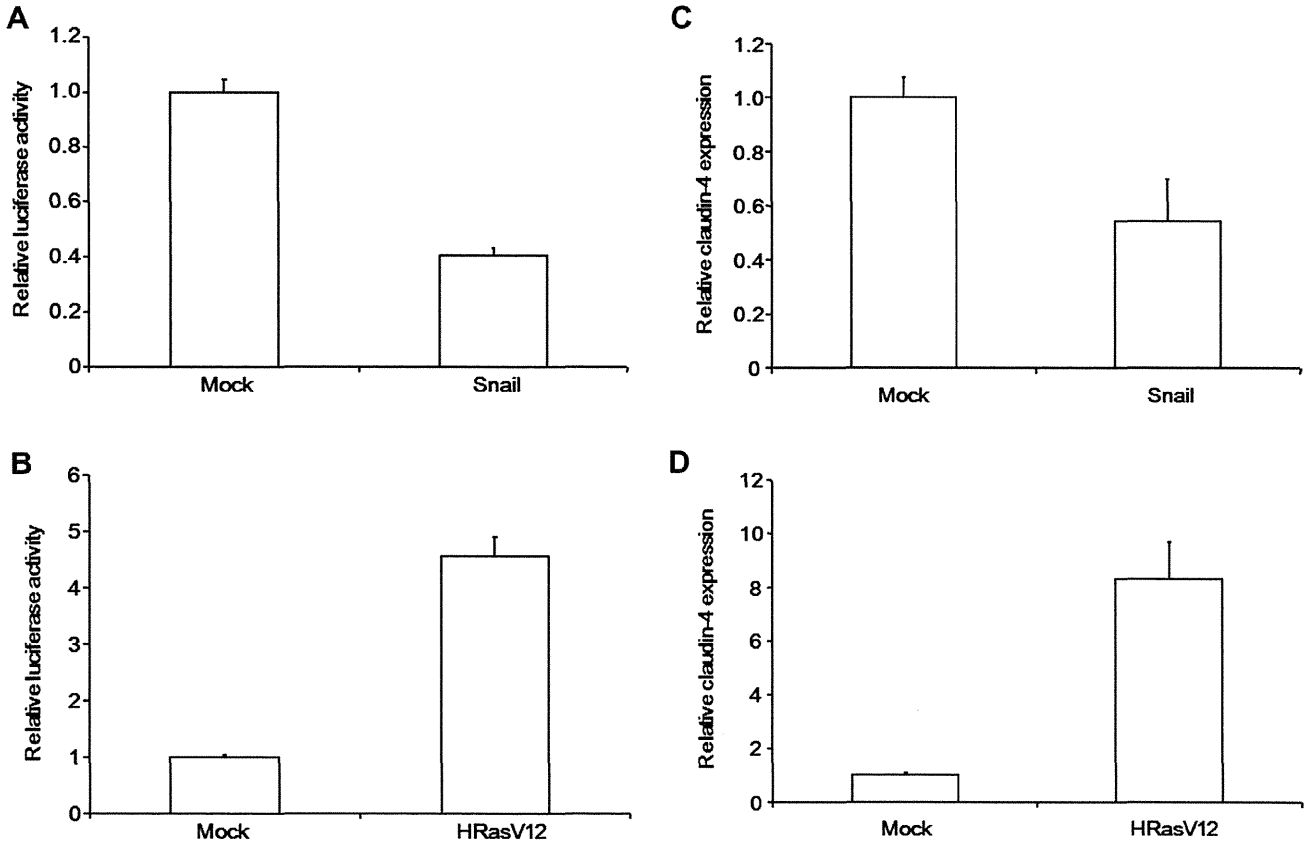

Fig. 1. Preparation of a reporter system monitoring claudin-4 expression. (A, B) Effects of snail and HRasV12 on the luciferase activity in transiently expressing cells. Snail-expressing MCF-7 cells (A) or HRasV12-expressing MCF7 cells (B) were transfected with the claudin-4 reporter plasmid. Two days later, the cells were recovered, and the luciferase activity in the lysates was measured. The data are means ± S.D. ($n = 3$). The results are representative of two independent experiments. (C, D) qPCR analysis of claudin-4 expression in transiently expressing cells. After 2 days of the transfection with the claudin-4 reporter plasmid, total RNA was extracted from snail-expressing MCF-7 cells (C) or HRasV12-expressing MCF-7 cells (D). Expression level of claudin-4 of the transfected cells was quantified by qPCR as described in the Section 2. Claudin-4 expression level was shown as ratio to that of the mock cells. The data are means ± S.D. ($n = 3$). The results are representative of two independent experiments.

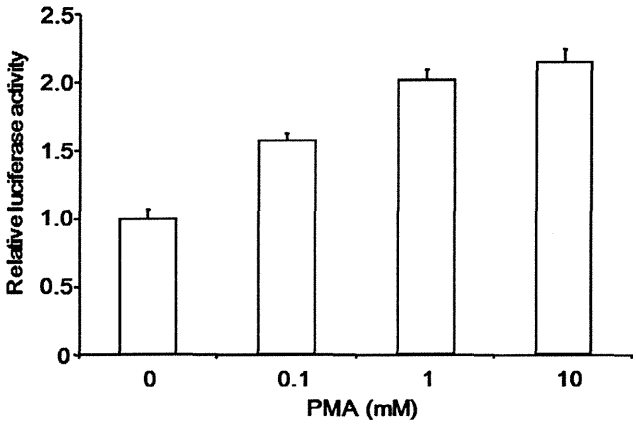

Fig. 2. Effect of PMA on the luciferase activity in clone 35 cells. Clone 35 cells were treated with PMA at the indicated concentrations for 24 h. Luciferase activity in the lysates was measured. The relative luciferase activity is shown as the ratio of the luciferase activity in the treated cells to that of the vehicle-treated cells. The data are means ± S.D. ($n = 3$). The results are representative of two independent experiments.

evaluate expression of the reporter gene, we checked the endogenous claudin-4 expression level in various cell lines and selected MCF-7, HaCat, HT1080, and SiHa cells, which have different claudin-4 expression levels for our analyses (Suppl. Fig. 1B). We transiently transfected the reporter plasmid into these cell lines and found that the luciferase activity of each was correlated with the endogenous expression level of claudin-4 (Suppl. Fig. 1C). We also investigated expression of the reporter gene in MCF-7 cells stably expressing snail or HRasV12, which suppress or induce claudin-4 expression, respectively [22,23]. Transfection of snail- or HRasV12-expressing MCF-7 cells with the reporter plasmid decreased or increased, respectively, the luciferase activity compared to that of mock-transfected MCF-7 cells (Fig. 1A and B). The difference in luciferase activity paralleled the level of claudin-4 mRNA in the cells (Fig. 1C and D), suggesting that the cloned promoter region was functional.

3.2. Preparation of a screening system for claudin-4 modulators

We transfected MCF-7 cells with the claudin-4 reporter plasmid and isolated stable transfected clones. We investigated the effect of transient expression of snail and HRasV12 on luciferase activity in these clones and found that several clones showed altered luciferase activity when transfected with the claudin-4 suppressor (snail, Suppl. Fig. 2A) or the claudin-4 inducer (HRasV12, Suppl. Fig. 2B). TGF-β suppresses claudin-4 expression [23], whereas EGF enhances claudin-4 expression [24]. Therefore, we also investigated the effects of TGF-β and EGF on the luciferase activity in the clones (Suppl. Fig. 2C and D, respectively). Since clone 35 showed the best

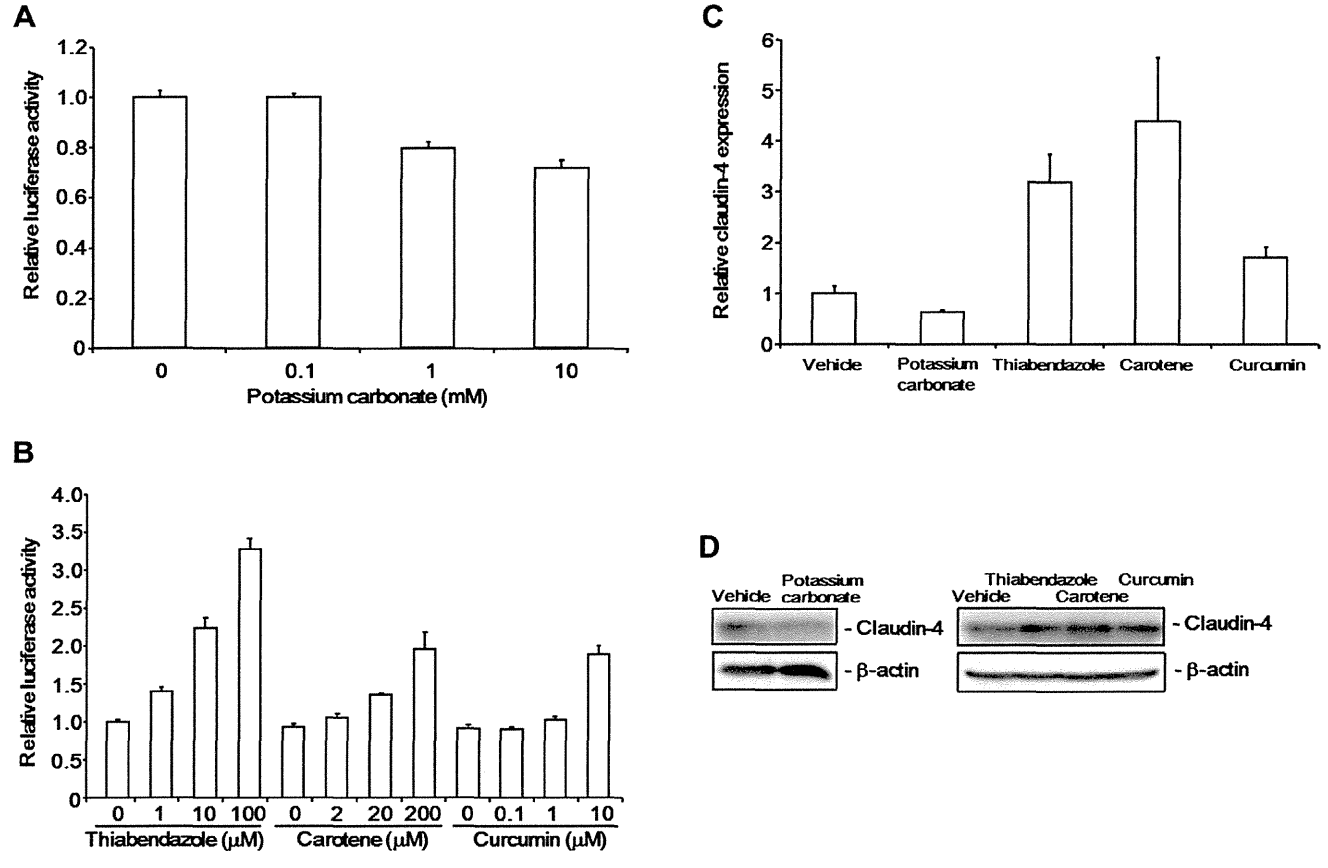

Fig. 3. Screening claudin-4 modulators using the reporter system. (A, B) Dose-dependent effects of the claudin-4 modulator candidates on luciferase expression. Clone 35 cells were treated with potassium carbonate (A), or thiabendazole, carotene, or curcumin (B) at the indicated concentrations for 24 h. Luciferase activity was measured in the lysates. Relative luciferase activity is shown as the ratio of the luciferase activity in the chemical-treated cells to that in the vehicle-treated cells. The data are means ± S.D. ($n = 3$). The results are representative of three independent experiments. (C, D) Effects of the claudin-4 modulator candidates on claudin-4 mRNA expression (C) and claudin-4 protein (D) levels. Clone 35 cells were treated with potassium carbonate (5 mM), thiabendazole (0.1 mM), carotene (0.2 mM), or curcumin (10 μM) for 24 h (C) or 48 h (D). Total RNA was used for qPCR analysis to detect claudin-4 mRNA (C). The relative mRNA expression of claudin-4 normalized to GAPDH expression. The cell lysates were subjected to SDS–PAGE, followed by immunoblotting for claudin-4 (D). GAPDH or β-actin served as loading controls. The result is representative of three independent experiments.

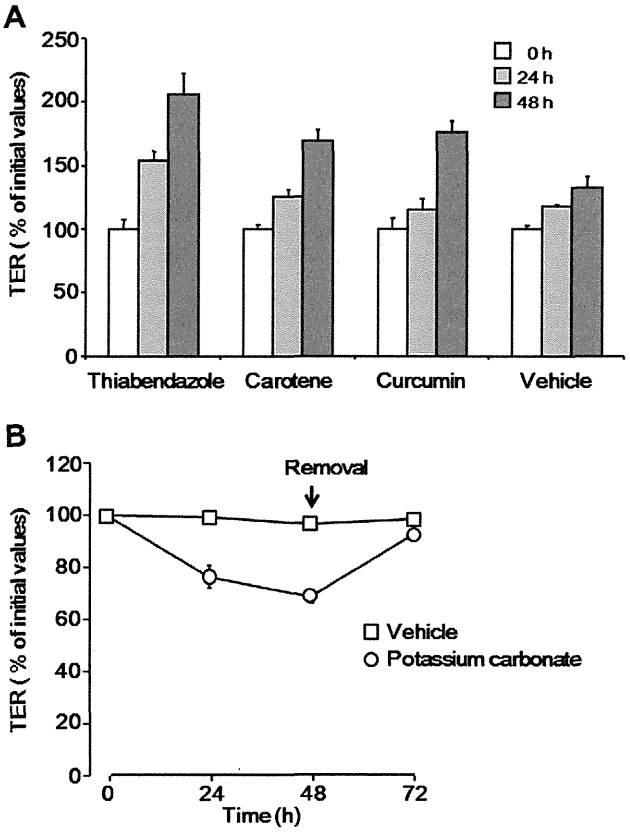

Fig. 4. Effects of claudin-4 modulator on the TJ-barrier in Caco-2 cells. (A) Effect of claudin-4 inducers on the TJ-barrier. Cells were seeded in Transwell™ chambers. Seven days after seeding, the cells were treated with thiabendazole (0.05 mM), carotene (0.2 mM), or curcumin (10 μM). TER values were monitored every 24 h. (B) Effect of a claudin-4 repressor on the TJ-barrier. Cells were seeded in Transwell™ chambers. When the TER values reached a plateau, the TJ-developed cells were treated with potassium carbonate (10 mM). After 48 h of treatment, the medium was replaced with fresh medium. The cells were then cultured for an additional 24 h. TER values were monitored every 24 h. TER values are shown as percentages of the TER values before treatment relative to those in treated cells, as described in the Section 2. The data are means ± S.D. ($n = 3$). These results are representative of three independent experiments.

response to the various claudin-4-modulating treatments, we selected it for further analysis. The clone 35 cells were treated with PMA, which enhances claudin-4 expression [25]. PMA increased luciferase activity in a dose-dependent manner (Fig. 2). These results indicate that clone 35 could be used to screen for modulators of claudin-4 expression.

3.3. Screening for claudin-4 modulators

When we eat, fragments of partially digested food, which still have antigenicity, exist in the intestine. This suggests that claudin modulators that tighten TJ-barriers may be contained in food. Therefore, we screened 86 chemicals used as food additives for claudin-4 modulators (Table 1). At first, we checked the cytotoxicity of these compounds in the clone 35 cells (Table 1). Then, we treated the cells with the compounds at non-toxic concentrations and identified the following claudin-4 modulator candidates: potassium carbonate (No. 3), thiabendazole (No. 68), carotene (No. 83), and curcumin (No. 86) (Suppl. Fig. 3). Each chemical modulated luciferase activity in a dose-dependent manner (Fig. 3A and B). qPCR analysis revealed that thiabendazole, carotene, and curcumin increased claudin-4 expression in the clone 35 cells (Fig. 3C), whereas potassium carbonate decreased claudin-4 expression. Similar results were obtained from Western blot analysis of claudin-4 (Fig. 3D).

To test whether the screened compounds also modulated the TJ-barrier, we investigated the effect of the compounds on the TER value, a marker of TJ-integrity, in Caco-2 cell monolayers, which is a popular model for mucosal barrier. Treatment of cells with thiabendazole, carotene, and curcumin increased the TER values (Fig. 4A). In contrast, potassium carbonate decreased the TER value. Moreover, the TER values recovered when the potassium carbonate was removed (Fig. 4B), and treatment with potassium carbonate did not cause cytotoxicity (data not shown). Thus, we successfully identified claudin-4 modulators.

4. Discussion

Claudin-4 inducers have been the focus of attention in drug development to treat inflammatory diseases and cancers [17–19]; however, their development has been slow. Some chemicals that modulate TJ integrity have been identified: glutamine, bryostatin-1, berberine, quercetin, and butyrate [26–30]. Here, we established a simple monitoring system for claudin-4 expression using a reporter gene, luciferase, and successfully identified chemical claudin-4 modulators: one suppressor of claudin-4 expression, potassium carbonate, and three inducers of claudin-4, thiabendazole, carotene, and curcumin.

Curcumin is an active ingredient of the spice turmeric, which is used in curry powders and as a food preservative. It is also used in traditional medicine to treat various inflammatory conditions, such as arthritis, colitis, and hepatitis [31]. Curcumin has various biological activities, such as anti-inflammatory, anti-oxidant, and anti-cancer effects [32]; however, the underlying mechanisms have never been fully understood. Here, we found that curcumin induces claudin-4 expression and increases TJ integrity. This enhancement of TJ integrity by curcumin may be associated with its therapeutic activities.

Carotene is a precursor of vitamin A. Retinoic acid, a metabolite of vitamin A, enhances TJ integrity in epithelial cells accompanied by expression of claudin-1, -4, and occludin [33]. These findings suggest that metabolized β-carotene-activated expression of claudins enhances the epithelial barrier in Caco-2 cells. Retinoic acid is a biologically active regulator of cell differentiation, proliferation, and apoptosis in various cell types [34]. The activities of retinoic acid are mediated by two types of nuclear receptors: retinoic acid receptors and their heterodimeric counterparts, retinoid X receptors [35]. Specific heterodimer-mediated transcriptional activation increases TJ integrity [36]. The increase in claudin-4 expression and TJ integrity induced by carotene may be caused by the formation of the heterodimer, followed by transcriptional activation.

Thiabendazole is used as a broad spectrum anthelmintic in various animal species and is also used to control parasitic infections in humans [37]. It is also used as an anti-fungal agent for the treatment of fruits [38]. Here, we found that thiabendazole increases claudin-4 expression and TJ integrity, but the mechanism for these activities remains unclear.

Our screening system identified a repressor of intestinal epithelial barrier function as well as three enhancers. We showed that potassium carbonate reduces claudin-4 expression and epithelial barrier function in Caco-2 cells without causing cytotoxicity. Potassium carbonate is used as an acidity regulator, and paracellular permeability is sensitive to pH [39]. Thus, potassium carbonate might reduce epithelial barrier integrity by changing the pH.

In conclusion, we developed the simple screening system for claudin-4 modulator, and we identified several claudin-4 modulators, including three inducers and one repressor. The screening system will thus be a tool for the development of claudin-4

modulators, thereby contributing to basic and pharmaceutical researches.

Acknowledgments

This work was supported by a Grant-in-Aid for Scientific Research from the Ministry of Education, Culture, Sports, Science, and Technology, Japan (21689006; 24390042), by a Health and Labor Sciences Research Grant from the Ministry of Health, Labor, and Welfare of Japan and by the Takeda Science Foundation.

Appendix A. Supplementary data

Supplementary data associated with this article can be found, in the online version, at http://dx.doi.org/10.1016/j.bbrc.2012.08.083.

References

[1] M. Cereijido, R.G. Contreras, L. Shoshani, D. Flores-Benitez, I. Larre, Tight junction and polarity interaction in the transporting epithelial phenotype, Biochim. Biophys. Acta 1778 (2008) 770–793.
[2] D.W. Powell, Barrier function of epithelia, Am. J. Physiol. 241 (1981) G275–288.
[3] A. Wodarz, I. Nathke, Cell polarity in development and cancer, Nat. Cell Biol. 9 (2007) 1016–1024.
[4] B.J. Aungst, Intestinal permeation enhancers, J. Pharm. Sci. 89 (2000) 429–442.
[5] M. Kondoh, T. Yoshida, H. Kakutani, K. Yagi, Targeting tight junction proteins-significance for drug development, Drug Discovery Today 13 (2008) 180–186.
[6] H. Chiba, M. Osanai, M. Murata, T. Kojima, N. Sawada, Transmembrane proteins of tight junctions, Biochim. Biophys. Acta 1778 (2008) 588–600.
[7] L.L. Mitic, V.M. Unger, J.M. Anderson, Expression, solubilization, and biochemical characterization of the tight junction transmembrane protein claudin-4, Protein Sci. 12 (2003) 218–227.
[8] M. Furuse, S. Tsukita, Claudins in occluding junctions of humans and flies, Trends Cell Biol. 16 (2006) 181–188.
[9] K. Morita, M. Furuse, K. Fujimoto, S. Tsukita, Claudin multigene family encoding four-transmembrane domain protein components of tight junction strands, Proc. Natl. Acad. Sci. USA 96 (1999) 511–516.
[10] M. Furuse, M. Hata, K. Furuse, Y. Yoshida, A. Haratake, Y. Sugitani, T. Noda, A. Kubo, S. Tsukita, Claudin-based tight junctions are crucial for the mammalian epidermal barrier: a lesson from claudin-1-deficient mice, J. Cell Biol. 156 (2002) 1099–1111.
[11] A. Gow, C.M. Southwood, J.S. Li, M. Pariali, G.P. Riordan, S.E. Brodie, J. Danias, J.M. Bronstein, B. Kachar, R.A. Lazzarini, CNS myelin and sertoli cell tight junction strands are absent in Osp/claudin-11 null mice, Cell 99 (1999) 649–659.
[12] T. Nitta, M. Hata, S. Gotoh, Y. Seo, H. Sasaki, N. Hashimoto, M. Furuse, S. Tsukita, Size-selective loosening of the blood–brain barrier in claudin-5-deficient mice, J. Cell Biol. 161 (2003) 653–660.
[13] P.J. Morin, Claudin proteins in human cancer: promising new targets for diagnosis and therapy, Cancer Res. 65 (2005) 9603–9606.
[14] J.D. Schulzke, S. Ploeger, M. Amasheh, A. Fromm, S. Zeissig, H. Troeger, J. Richter, C. Bojarski, M. Schumann, M. Fromm, Epithelial tight junctions in intestinal inflammation, Ann. N. Y. Acad. Sci. 1165 (2009) 294–300.
[15] N. Sonoda, M. Furuse, H. Sasaki, S. Yonemura, J. Katahira, Y. Horiguchi, S. Tsukita, *Clostridium perfringens* enterotoxin fragment removes specific claudins from tight junction strands: evidence for direct involvement of claudins in tight junction barrier, J. Cell Biol. 147 (1999) 195–204.
[16] H. Uchida, M. Kondoh, T. Hanada, A. Takahashi, T. Hamakubo, K. Yagi, A claudin-4 modulator enhances the mucosal absorption of a biologically active peptide, Biochem. Pharmacol. 79 (2010) 1437–1444.
[17] R. Mennigen, K. Nolte, E. Rijcken, M. Utech, B. Loeffler, N. Senninger, M. Bruewer, Probiotic mixture VSL#3 protects the epithelial barrier by maintaining tight junction protein expression and preventing apoptosis in a murine model of colitis, Am. J. Physiol. 296 (2009) G1140–1149.
[18] S.K. Lee, J. Moon, S.W. Park, S.Y. Song, J.B. Chung, J.K. Kang, Loss of the tight junction protein claudin 4 correlates with histological growth-pattern and differentiation in advanced gastric adenocarcinoma, Oncol. Rep. 13 (2005) 193–199.
[19] S. Mima, S. Tsutsumi, H. Ushijima, M. Takeda, I. Fukuda, K. Yokomizo, K. Suzuki, K. Sano, T. Nakanishi, W. Tomisato, T. Tsuchiya, T. Mizushima, Induction of claudin-4 by nonsteroidal anti-inflammatory drugs and its contribution to their chemopreventive effect, Cancer Res. 65 (2005) 1868–1876.
[20] H. Honda, M.J. Pazin, H. Ji, R.P. Wernyj, P.J. Morin, Crucial roles of Sp1 and epigenetic modifications in the regulation of the CLDN4 promoter in ovarian cancer cells, J. Biol. Chem. 281 (2006) 21433–21444.
[21] T. Vincent, E.P. Neve, J.R. Johnson, A. Kukalev, F. Rojo, J. Albanell, K. Pietras, I. Virtanen, L. Philipson, P.L. Leopold, R.G. Crystal, A.G. de Herreros, A. Moustakas, R.F. Pettersson, J. Fuxe, A SNAIL1-SMAD3/4 transcriptional repressor complex promotes TGF-beta mediated epithelial–mesenchymal transition, Nat. Cell Biol. 11 (2009) 943–950.
[22] J. Ikenouchi, M. Matsuda, M. Furuse, S. Tsukita, Regulation of tight junctions during the epithelium–mesenchyme transition: direct repression of the gene expression of claudins/occludin by snail, J. Cell Sci. 116 (2003) 1959–1967.
[23] P. Michl, C. Barth, M. Buchholz, M.M. Lerch, M. Rolke, K.H. Holzmann, A. Menke, H. Fensterer, K. Giehl, M. Lohr, G. Leder, T. Iwamura, G. Adler, T.M. Gress, Claudin-4 expression decreases invasiveness and metastatic potential of pancreatic cancer, Cancer Res. 63 (2003) 6265–6271.
[24] A. Ikari, K. Atomi, A. Takiguchi, Y. Yamazaki, M. Miwa, J. Sugatani, Epidermal growth factor increases claudin-4 expression mediated by Sp1 elevation in MDCK cells, Biochem. Biophys. Res. Commun. 384 (2009) 306–310.
[25] C. Wray, Y. Mao, J. Pan, A. Chandrasena, F. Piasta, J.A. Frank, Claudin-4 augments alveolar epithelial barrier function and is induced in acute lung injury, Am. J. Physiol. 297 (2009) L219–227.
[26] L. Gu, N. Li, Q. Li, Q. Zhang, C. Wang, W. Zhu, J. Li, The effect of berberine in vitro on tight junctions in human Caco-2 intestinal epithelial cells, Fitoterapia 80 (2009) 241–248.
[27] N. Li, V.G. DeMarco, C.M. West, J. Neu, Glutamine supports recovery from loss of transepithelial resistance and increase of permeability induced by media change in Caco-2 cells, J. Nutr. Biochem. 14 (2003) 401–408.
[28] L. Peng, Z.R. Li, R.S. Green, I.R. Holzman, J. Lin, Butyrate enhances the intestinal barrier by facilitating tight junction assembly via activation of AMP-activated protein kinase in Caco-2 cell monolayers, J. Nutr. 139 (2009) 1619–1625.
[29] T. Suzuki, H. Hara, Quercetin enhances intestinal barrier function through the assembly of zonula [corrected] occludens-2, occludin, and claudin-1 and the expression of claudin-4 in Caco-2 cells, J. Nutr. 139 (2009) 965–974.
[30] J. Yoo, A. Nichols, J.C. Song, J. Mammen, I. Calvo, R.T. Worrell, J. Cuppoletti, K. Matlin, J.B. Matthews, Bryostatin-1 attenuates TNF-induced epithelial barrier dysfunction: role of novel PKC isozymes, Am. J. Physiol. 284 (2003) G703–712.
[31] J. Epstein, I.R. Sanderson, T.T. Macdonald, Curcumin as a therapeutic agent: the evidence from in vitro, animal and human studies, Br. J. Nutr. 103 (2010) 1545–1557.
[32] R.K. Maheshwari, A.K. Singh, J. Gaddipati, R.C. Srimal, Multiple biological activities of curcumin: a short review, Life Sci. 78 (2006) 2081–2087.
[33] M. Osanai, N. Nishikiori, M. Murata, H. Chiba, T. Kojima, N. Sawada, Cellular retinoic acid bioavailability determines epithelial integrity: role of retinoic acid receptor alpha agonists in colitis, Mol. Pharmacol. 71 (2007) 250–258.
[34] M. Osanai, M. Petkovich, Expression of the retinoic acid-metabolizing enzyme CYP26A1 limits programmed cell death, Mol. Pharmacol. 67 (2005) 1808–1817.
[35] P. Kastner, M. Mark, P. Chambon, Nonsteroid nuclear receptors: what are genetic studies telling us about their role in real life?, Cell 83 (1995) 859–869
[36] H. Kubota, H. Chiba, Y. Takakuwa, M. Osanai, H. Tobioka, G. Kohama, M. Mori, N. Sawada, Retinoid X receptor alpha and retinoic acid receptor gamma mediate expression of genes encoding tight-junction proteins and barrier function in F9 cells during visceral endodermal differentiation, Exp. Cell Res. 263 (2001) 163–172.
[37] K. Walton, R. Walker, J.J. van de Sandt, J.V. Castell, A.G. Knapp, G. Kozianowski, M. Roberfroid, B. Schilter, The application of in vitro data in the derivation of the acceptable daily intake of food additives, Food Chem. Toxicol. 37 (1999) 1175–1197.
[38] J.P. Groten, W. Butler, V.J. Feron, G. Kozianowski, A.G. Renwick, R. Walker, An analysis of the possibility for health implications of joint actions and interactions between food additives, Regul. Toxicol. Pharmacol. 31 (2000) 77–91.
[39] V.W. Tang, D.A. Goodenough, Paracellular ion channel at the tight junction, Biophys. J. 84 (2003) 1660–1673.

Original Article

Novel TNF-α Receptor 1 Antagonist Treatment Attenuates Arterial Inflammation and Intimal Hyperplasia in Mice

Manabu Kitagaki[1], Kikuo Isoda[2], Haruhiko Kamada[3], Takayuki Kobayashi[4], Shinichi Tsunoda[3], Yasuo Tsutsumi[3,5], Tomiharu Niida[2], Takehiko Kujiraoka[2], Norio Ishigami[2], Miya Ishihara[1], Osamu Matsubara[4], Fumitaka Ohsuzu[2] and Makoto Kikuchi[1]

[1]Medical Engineering, National Defense Medical College, Saitama, Japan
[2]Internal Medicine I, National Defense Medical College, Saitama, Japan
[3]Laboratory of Biopharmaceutical Research, National Institute of Biomedical Innovation, Osaka, Japan
[4]Basic Pathology, National Defense Medical College, Saitama, Japan
[5]Department of Toxicology and Safety Science, Graduate School of Pharmaceutical Sciences, Osaka University, Osaka, Japan

Aim: **Tumor necrosis factor receptor 1 (TNFR1) participates importantly in arterial inflammation in genetically altered mice; however it remains undetermined whether a selective TNFR1 antagonist inhibits arterial inflammation and intimal hyperplasia. This study aimed to determine the effect and mechanism of a novel TNFR1 antagonist in the suppression of arterial inflammation.**
Methods: **We investigated intimal hyperplasia in IL-1 receptor antagonist-deficient mice two weeks after inducing femoral artery injury in an external vascular cuff model. All mice received intraperitoneal injections of TNFR1 antagonist (PEG-R1antTNF) or normal saline twice daily for 14 days.**
Results: **PEG-R1antTNF treatment yielded no adverse systemic effects, and we observed no significant differences in serum cholesterol or blood pressure in either group; however, selective PEG-R1antTNF treatment significantly reduced intimal hyperplasia (19,671±4,274 vs. 11,440±3,292 μm^2; $p=0.001$) and the intima/media ratio (1.86±0.43 vs. 1.34±0.36; $p=0.029$), compared with saline injection. Immunostaining revealed that PEG-R1antTNF inhibits Nuclear factor-κB (NF-κB), suppressing smooth muscle cell (SMC) proliferation and decreasing chemokine and adhesion molecule expression, and thus decreasing intimal hyperplasia and inflammation.**
Conclusions: **Our data suggest that PEG-R1antTNF suppresses SMC proliferation and inflammation by inhibiting NF-κB. This study highlights the potential therapeutic benefit of selective TNFR1 antagonist therapy in preventing intimal hyperplasia and arterial inflammation.**

J Atheroscler Thromb, 2012; 19:36-46.

Key words; TNF receptor 1 antagonist, Cytokine, Inflammation, Intimal hyperplasia, Smooth muscle cell

Introduction

Tumor necrosis factor-α (TNF-α) possesses important proinflammatory properties that participate crucially in innate and adaptive immunity[1]. Due to its numerous effects on different cell types (e.g., macrophages, endothelial cells, and smooth muscle cells (SMCs)), TNF-α might contribute to arterial inflammation and intimal hyperplasia, including the induction of adhesion molecule expression of cell migration and proliferation[2,3].

TNF-α elicits responses through two receptors, TNF receptor 1 (TNFR1) and TNF-α receptor 2 (TNFR2). TNFR1 activates the majority of biological responses[4]. TNFR2 is mainly expressed in cells associated with the immune response, and TNFR2 signaling plays an important role in the biophylactic system[5]. Several previous studies have examined the effect of TNFR1 signaling on vascular physiology using TNFR1-deficient mice. Schreyer *et al.* demonstrated

Address for correspondence: Kikuo Isoda, Internal Medicine I, National Defense Medical College, 3-2, Namiki, Tokorozawa, Saitama, 359-8513, Japan
E-mail: isoda@ndmc.ac.jp
Received: April 18, 2011
Accepted for publication: August 9, 2011

an anti-atherogenic effect of TNFR1 signaling[6]. In another study, TNFR1 did not affect atherosclerosis in Apo E-deficient mice[7]. Conversely, Zhang *et al.* demonstrated that TNFR1 expression in the arterial wall contributed substantially to atherosclerosis in an arterial grafting model using TNFR1-deficient mice[8]. Furthermore, they demonstrated that TNF signaling via TNFR2 attenuated neointimal hyperplasia by reducing adhesion molecule expression and endothelial cell apoptosis in an arterial grafting model using TNFR2-deficient mice[9]. Xanthoulea *et al.* showed that atherosclerotic plaques are smaller in LDL receptor-deficient mice carrying TNFR1-deficient bone marrow compared to controls[10]. Taken together, these studies suggest that the role of TNF-α, TNFR1 and TNFR2 in vascular inflammation remains incompletely understood. As referred to above, several reports using genetically-altered mice suggested that TNFR1-specific blocking therapy may be the optimal therapy for arterial inflammation; however, no current data show that blocking with a TNFR1 antagonist contributes to the inhibition of arterial inflammation and atherogenesis. We therefore attempted to reveal the roles of these two TNF receptor subtypes in arterial inflammation *in vitro* and *in vivo* using a TNFR1 antagonist.

Recently, two types of TNF blocker, infliximab (chimeric TNF-α monoclonal antibody) and etanercept (soluble TNF receptor), have become available for the treatment of rheumatoid arthritis, and have proven to be efficacious. Previous reports showed that anti-TNF therapy improved endothelial function and decreased cardiovascular events associated with systemic inflammation of rheumatoid arthritis[11-13], but the therapy has its downsides. Inhibition of TNF-α function by anti-TNF therapy increases the chance of infection[14], whereas TNFR1-specific blocking therapy (inhibiting only TNFR1 signal, but not TNFR2 signal) has the potential to inhibit inflammation and offset the side effects of conventional TNF blockers.

More recently, our colleagues produced a novel TNFR1-selective antagonistic mutant TNF-α (R1antTNF) using phage display[15], and also developed PEGylated R1antTNF (PEG-R1antTNF), an agent that further enhances potential anti-inflammatory activity[16, 17]. The aim of the present study, therefore, was to clarify the effect of this novel TNFR1 antagonist on arterial inflammation and intimal hyperplasia.

Materials and Methods

Novel Tumor Necrosis Factor-α Receptor 1 Antagonist; R1antTNF and PEG-R1antTNF

Our colleagues developed R1antTNF and PEG-R1antTNF for use with a phage-display system. Briefly, they constructed a phage library that displays structural variants of human TNF, in which random amino acid sequences replace the 6 residues (amino acids 84-89) that are likely present in the TNF receptor-binding site from the crystal structure of the LT-α-TNFR1 complex. This phage library consisted of 1×10^7 independent recombinant clones. The phage selection that displays structural TNF variants (Panning) yielded the structural TNF variant R1antTNF with selectively high affinity for TNFR1 and inhibition of TNFR1 signaling. Compared with wild-type TNF-α, R1antTNF has superior affinity for TNFR1, but only one fifty-thousandth of affinity for TNFR2. PEG-R1antTNF is PEGylated R1antTNF, which PEG (polyethylene glycol; average molecular weigh 5,000) binds to N-terminal site of R1antTNF, thus improving circulatory retention[15-17].

To compare *in vivo* stability, we injected mice intraperitoneally with PEG-R1antTNF and R1antTNF, and measured serum levels at the indicated time points. In the R1antTNF group, serum concentration almost attained the limit of detection 12 h post-injection. In contrast, the retention time of PEG-R1antTNF in the circulation was considerably longer than R1antTNF[17].

Cell Culture

We purchased human umbilical vein endothelial cells (HUVECs) and human aortic smooth muscle cells (HASMCs) (Kurabo). After culturing HUVECs in HuMedia-EG2 and HASMCs in HuMedia-SG2 (Kurabo) with growth factor, fourth and seventh passage cells, respectively, were used for our experiment. HUVECs and HASMCs were cultured to confluence. After washing the dishes, HUVECs and HASMCs were cultured with 1 ng/mL human recombinant TNF-α (R&D systems) and 1 μg/mL R1antTNF for 5, 10, 30, 60 and 120min. The cells were lysed with Lysis Buffer (50 mM Tris-HCl, 150 mM NaCl, 1 mM EDTA, 1% TritonX-100, 50 mM NaF, 30 mM $Na_4O_7P_2$, 1 mM Na_3VO_4, protease inhibitor) and used for Western blotting.

SDS-PAGE and Western Blotting

Cell lysate and 2x protein sample buffer for SDS-PAGE (BIO-RAD) were mixed equally, and then 2-mercaptethanol was added at a final concentration

of 5%. After incubation at 100℃ for 10min, these samples were separated by 10-20% SDS-PAGE and transferred to a polyvinylidene difluoride (PVDF) membrane (Hoefer). The membrane was incubated with rabbit anti-phospho-nuclear factor-kappa B (pNF-κB) (Cell Signaling) diluted 1:1000, rabbit anti-phospho-endothelial/epithelial tyrosine kinase (pEtk) (Cell Signaling) diluted 1:1000 and mouse anti-human β-actin (BD Bioscience) diluted 1:30000 in 4% BlockAce (Dainippon Sumitomo Pharma), and then treated with goat anti-rabbit IgG-horseradish peroxidase (Cell Signaling) diluted 1:2000 and goat anti-mouse IgG-horseradish peroxidase (Sigma Aldrich) diluted 1:50000, respectively. Immunodetection was performed with chemiluminescent reagent; ECL-plus (GE Healthcare). The immunoblot was analyzed with an imaging system (LAS3000; Fuji Film), and bands density was estimated using Image J 1.14 (National Institutes of Health).

Reverse Transcription Quantitative PCR *in vitro*

We cultured HUVECs with 1 ng/mL human recombinant TNFα (R&D Systems) and 1 μg/mL R1antTNF for 24 hours. Total RNA from HUVECs was isolated with TRIzol (Invitrogen). Complimentary DNA was obtained using SuperScript Ⅲ Reverse Transcriptase (Invitrogen) according to the manufacturer's instructions. Quantitative mRNA expression was assessed by real-time PCR with Taqman PCR Master Mix (Applied Biosystems) using specific primers for ICAM-1 (Taqman gene expression assay; Applied Biosystems). Samples were run in duplicate on the 7900HT Fast Real-Time OCR system (Applied Biosystems).

Mice and Genotyping

Interleukin-1 receptor antagonist deficiency (IL-1Ra-/-) mice were generated in our laboratory by replacing the exons encoding the secreted form with the neo gene, as previously described[18]. IL-1Ra-/- mice showed excessive arterial inflammation and intimal hyperplasia after cuff injury[19].

Embryonic stem cells were aggregated with 2 (C57BL6J × DBA/2) F1 mice at the 8-cell stage. All 4 isoforms of IL-1Ra were destroyed and mutant mice were a background to C57BL/6J strain mice for 8 generations. To obtain homozygous mutant mice, heterozygous mice were intercrossed with each other. All studies were conducted according to the protocols approved by the National Defense Medical College Board for Studies in Experimental Animals.

Femoral Artery Injury and Treatment

To eliminate gender differences, we used only male mice. Eight-week-old mice were anesthetized by intraperitoneal injection of pentobarbital (50 mg/kg). We dissected the left femoral artery from its surrounding, as described previously[20]. Vascular injury was inflicted by placing a non-occlusive polyethylene cuff (length 2.0 mm; internal diameter 0.56 mm; Becton Dickinson) around the femoral artery. Mice received intraperitoneal injections of PEG-R1antTNF (experimental model; 3 μg twice daily) or normal saline (controls) twice daily for two weeks.

Plasma Lipid Measurement

A blood sample was collected from both groups at 14 days post-injury. Plasma total cholesterol, low-density lipoprotein (LDL) cholesterol, and high-density lipoprotein (HDL) cholesterol levels were measured by high performance liquid chromatography (HPLC) at Skylight Biotech Inc. (Akita, Japan) as described previously[21]. Plasma lipoproteins were analyzed by an on-line dual enzymatic method for simultaneous quantification of cholesterol according to the procedure described by Usui *et al.*[22].

Arterial Harvest and Morphometric Analysis

After measuring systolic blood pressure, the animals were euthanized by pentobarbital injection and the vascular tree perfused with 0.9% NaCl followed by 4% paraformaldehyde. Following perfusion, the femoral artery was harvested and fixed with 10% neutral-buffered formalin.

We embedded the artery in paraffin and cut 10 sections (each 5-μm thick) from 10 equally spaced locations. The slides were stained with hematoxylin-eosin and elastica van Gieson, and then examined and photographed using ECLIPS LV100 microscopy (Nikon). The luminal, neointimal, and medial areas were calculated using NIS element (Nikon). To determine the effect of PEG-R1antTNF on vascular remodeling, we defined the vessel area as the area inside external elastic lamina, and calculated the intima area/vessel area ratio.

Immunohistochemistry

Using anti-proliferating cell nuclear antigen (PCNA) antibody (1:100; Dako), α smooth muscle actin (SMA) antibody (Dako), and pNF-κB antibody (1:50; Santa Cruz Biotechnology, Santa Cruz), respectively, we conducted immunohistochemistry for proliferating, SMCs, and NF-κB activation on paraffin-embedded sections. Before immunostaining, sections were treated in a microwave oven in 0.1 mol/L citrate

buffer, pH 6.0. Endogenous peroxidase was blocked by incubation with 3% H_2O_2 in methanol for 5 min. Slides were incubated with normal swine serum (Vector Laboratories) for 10 minutes and then with primary antibody overnight at 4℃ at the concentrations described above. The sections were incubated with the complementary secondary antibody for 60 min. We visualized the sections using the Envison system (Dako) with DAB as the substrate. Conversely, we conducted immunohistochemistry on frozen sections of monocytes/macrophages, leukocyte adhesion molecules, and chemokines, using anti-CD11b antibody (1:50; BD Bioscience), anti-intracellular adhesion molecule 1 (ICAM-1) antibody (1:50 R&D Systems), and monocyte chemoattractant protein 1 (MCP-1) antibody (1:100; Santa Cruz Biotechnology), respectively. The secondary antibody was the biotinylated antibody (Dako). The sections were visualized with a Vectastain ABC kit (Vector Laboratories), using DAB as the substrate. The nuclei were counterstained with Mayer's hematoxylin solution. Negative control slides were incubated without a primary antibody.

Reverse Transcription Quantitative PCR

Total RNA from the liver, lung, thymus gland and femoral artery tissue was isolated with TRIzol (Invitrogen). Complimentary DNA was obtained using SuperScript Ⅲ Reverse Transcriptase (Invitrogen) according to the manufacturer's instructions. Quantitative mRNA expression was assessed by real-time PCR with Power SYBR Green PCR Master Mix (Applied Biosysytems) using primers specific for TNF-α (forward: TCC CAG GTT CTC TTC AAG GGA, reverse: GGT GAG GAG CAC GTA GTC GG), MCP-1 (forward: CCA CTC ACC TGC TAC TCA T, reverse: TGGTGA TCC TCTTGT AGC TCT CC) and GAPDH (forward: AAC TTT GGC ATT GTG GAA GG, reverse: ACA CAT TGG GGG TAG GAA CA). Samples were run in duplicate on the 7900HT Fast Real-Time PCR system (Applied Biosystems).

Statistical Analysis

Results are shown as the mean ± SD. Differences between groups were analyzed by Student's t test. $P<0.05$ was regarded as significant.

Results

R1antTNF Limited TNFα Induced NF-κB Activation in Endothelial Cells and Smooth Muscle Cells

Western blotting was used to examine pNF-κB expression in HUVECs and SMCs to ascertain whether R1antTNF inhibited TNFR1 signaling. pNF-κB peaked 30min after TNF-α stimulation and then deteriorated quickly. R1antTNF decreased pNF-κB expression in both HUVECs and SMCs compared with the control (**Fig. 1A**). Calculation of the pNF-κB/β-actin expression ratio 30 min after TNF-α stimulation showed that R1antTNF inhibition of pNF-κB expression was superior to the control in HUVECs (2.03 ± 0.57 vs. 1.30 ± 0.08: $p=0.045$) and SMCs (1.74 ± 0.16 vs. 1.17 ± 0.26: $p=0.009$) (**Fig. 1B**).

To determine the influence on TNFR2 signaling, we investigated the specific effect of phosphorylated pEtk on TNFR2 signaling. pEtk peaked 5 min after TNF-α stimulation in endothelial cells. We observed no significant differences in pEtk expression between groups (**Fig. 1C**).

Next, we evaluated mRNA levels of ICAM-1 in HUVECs using real-time PCR. Analysis revealed the reduction of mRNA levels of ICAM-1 in HUVECs with both TNF-α and R1antTNF compared with those with TNF-α only (2.11 ± 0.38 vs. 1.54 ± 0.23; $p=0.042$) (**Fig. 2**).

PEG-R1antTNF Treatment Yielded No Adverse in IL-1Ra-/- Mice

We investigated intimal hyperplasia in IL-1Ra-/- mice two weeks after femoral artery injury by an external vascular cuff model. Mice received intraperitoneal injections of PEG-R1antTNF (experimental model) or normal saline (controls) twice daily for two weeks. No adverse systemic effects of PEG-R1antTNF were observed and systolic blood pressure was similar between groups (**Table 1**). Moreover, plasma lipid analysis revealed no statistically significant differences in total cholesterol, LDL cholesterol, and HDL cholesterol between these groups (**Table 2**).

To examine how R1antTNF influences the whole body, we evaluated TNF-α mRNA expression levels in the liver, lung, and thymus gland two weeks after administration using reverse transcription quantitative PCR. We observed a tendency toward inhibited TNF-α mRNA expression in the liver of the PEG-R1antTNF group, but the difference was not statistically significant compared with controls (1.98 ± 1.41 vs. 0.66 ± 0.33: $p=0.075$). Expression levels of TNF-α mRNA in the lung and thymus gland of the PEG-R1antTNF group did not differ significantly from the controls (**Table 3**).

PEG-R1antTNF Inhibited Intimal Hyperplasia in IL-1Ra-/- Arteries Post-Injury

We investigated the effect of PEG-R1antTNF treatment on the femoral arteries of IL-1Ra-/- mice following cuff-induced injury. **Fig. 3** shows representa-

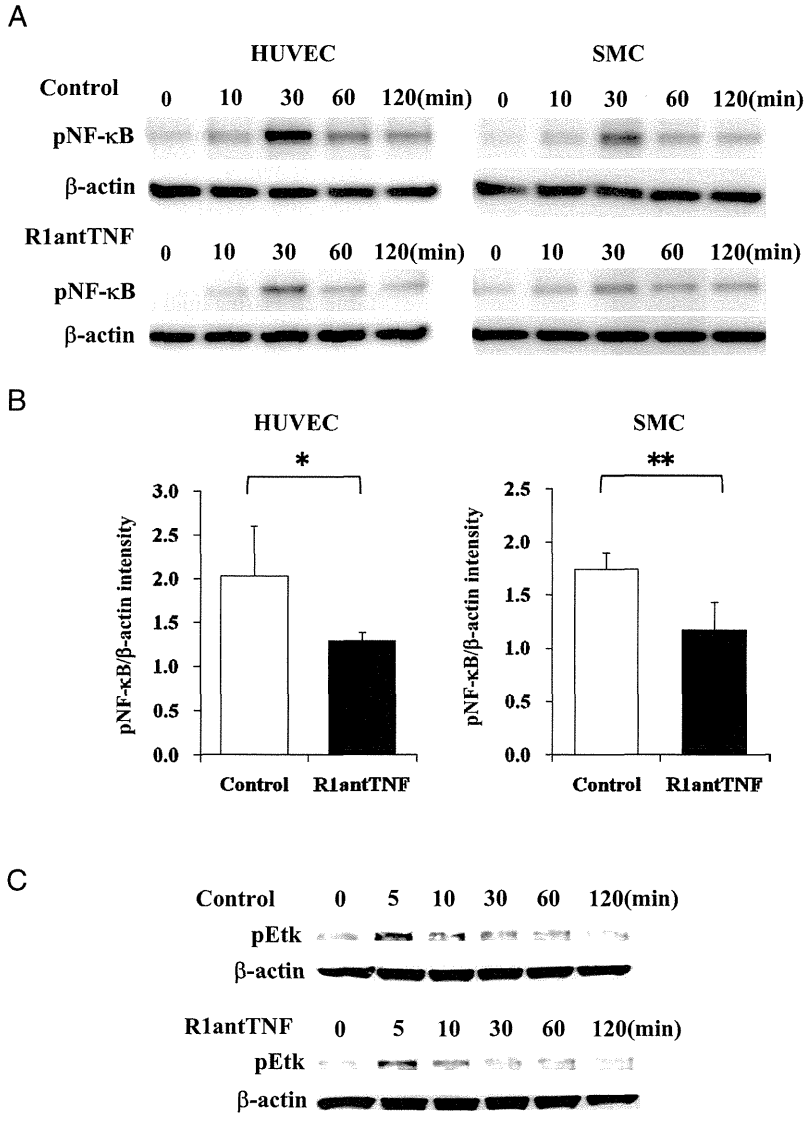

Fig. 1. R1antTNF significantly inhibited the expression of pNF-κB in HUVECs and SMCs.

(A) Expression levels of pNF-κB peaked 30 min after stimulation in Western blot analysis. (B) Bar graphs show band density 30 min after stimulation in control and R1antTNF treatment. Data are expressed as the mean ± SD ($n=4$). *$p<0.05$, **$p<0.01$. (C) There was no difference in the expression levels of pEtk between R1antTNF and the control group in Western blot analysis.

tive cross sections of femoral arteries harvested 14 days post-injury. Immunostaining for α-SMA showed that intimal hyperplasia consisted of SMCs. PEG-R1antTNF but not saline treatment inhibited intimal hyperplasia (**Fig. 3A**). Morphometric analysis revealed significantly decreased intimal hyperplasia in mice receiving PEG-R1antTNF treatment compared with controls (19,671 ± 4,274 vs. 11,440 ± 3,292 μm^2; $p=0.001$) (**Fig. 3B**). PEG-R1antTNF treatment also decreased the intima/media ratio (1.86 ± 0.43 vs. 1.34 ± 0.36; $p=0.029$) and the intima/vessel area ratio (0.35 ± 0.06 vs. 0.21 ± 0.11; $p=0.011$) compared with saline controls (**Fig. 3C** and **D**); therefore, our results suggest that PEG-R1antTNF significantly decreases intimal hyperplasia.

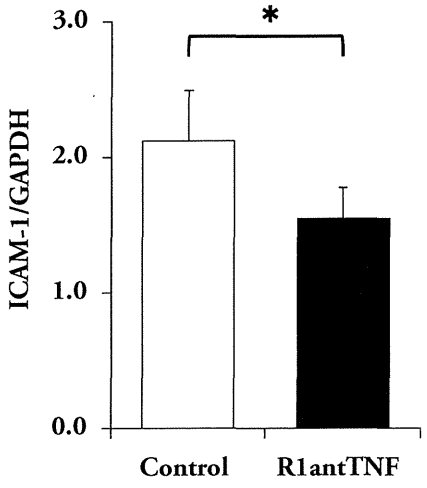

Fig. 2. R1antTNF inhibited the expression of ICAM-1 mRNA in HUVECs after TNF-α stimulation. mRNA levels of ICAM-1 were assessed with real-time PCR. Data are expressed as the mean ± SD ($n=4$). *$p<0.05$.

Inhibition of NF-κB Activation by PEG-R1antTNF Decreased Expression of Chemokine and Adhesion Molecule

To examine TNF-α and MCP-1 expression in the injured artery 5 days post-surgery, real-time PCR was performed to evaluate mRNA levels of TNF-α and MCP-1. Mice receiving PEG-R1antTNF treatment showed inhibited expression of TNF-α (2.62 ± 1.47 vs. 1.06 ± 0.74; $p=0.029$) and MCP-1 (1.34 ± 0.77 vs. 0.50 ± 0.24; $p=0.048$) mRNA compared with control mice (**Fig. 4A**).

To determine the effect of PEG-R1antTNF on injured arteries, immunostaining for pNF-κB was performed at 7 and 14 days post-injury. Fewer pNF-κB- positive nuclei were observed in the intima of PEG-R1antTNF-treated mice at 7 and 14 days than in controls (**Fig. 4B**). ICAM-1 and MCP-1 expressions were also investigated, and both increased in endothelial cells from controls but not PEG-R1antTNF-treated mice (**Fig. 4C**). Immunostaining also revealed fewer macrophages in the intima of PEG-R1antTNF-treated mice than in controls (**Fig. 4C**).

To determine cell proliferating activity, immunostaining for PCNA was performed 14 days post-injury. PEG-R1antTNF decreased the number of PCNA-positive nuclei compared with controls. Furthermore, the expression of PCNA-positive nuclei considerably accorded with α-SMA-positive cells (**Fig. 5A**). Quantitative analysis also revealed that PEG-R1antTNF-treated mice had fewer PCNA-positive nuclei than controls 14 days post-injury (**Fig. 5B**). These data suggest that PEG-R1antTNF exerts a vascular anti- inflammatory effect by inhibiting NF-κB.

Table 1. Measurement of blood pressure and heart rate at 14 days post-injured

	Control	R1antTNF	p value
Blood pressure (mmHg)	106.6 ± 10.0	110.6 ± 5.3	0.451
Heart rate (bpm)	654.2 ± 48.6	666.6 ± 56.9	0.721

Results are expressed as the mean ± SD

Table 2. Plasma lipid analysis at 14 days post-injured

	Control	R1antTNF	p value
Total Cholesterol (mg/dL)	73.11 ± 8.30	68.87 ± 8.37	0.399
LDL Cholesterol (mg/dL)	21.69 ± 4.47	18.37 ± 2.33	0.137
HDL Cholesterol (mg/dL)	46.73 ± 6.75	44.79 ± 9.02	0.683

Results are expressed as the mean ± SD

Table 3. TNF-α mRNA expression at 14 days post-injured

	Control	R1antTNF	p value
Liver	1.98 ± 1.41	0.66 ± 0.33	0.075
Lung	1.10 ± 0.18	1.10 ± 0.74	0.994
Thymus Gland	0.98 ± 0.53	1.09 ± 0.32	0.728

Value is TNF-α mRNA/GAPDH mRNA ratio. Results are expressed as the mean ± SD

Discussion

We demonstrate here for the first time that a specific TNFR1 antagonist inhibited intimal hyperplasia following arterial inflammation induced by cuff injury in IL-1Ra-/- mice with excessive post-injury inflammation. Previous reports demonstrated that TNFR1 participates in exacerbated intimal hyperplasia in wire-injured artery[23] or arteriovenous grafts[8] using the mouse carotid artery. Moreover, a study using double-deficient (TNFR1 and LDL receptor) mice showed decreasing sizes of atherosclerotic plaque[24]. Thus, TNF-α plays an important role, and TNF signaling through TNFR1 participates significantly in the development of intimal hyperplasia and atherosclerosis; however, these findings were observed in genetically altered mice, and the current literature does not show how the TNFR1 antagonist might affect arterial inflammation.

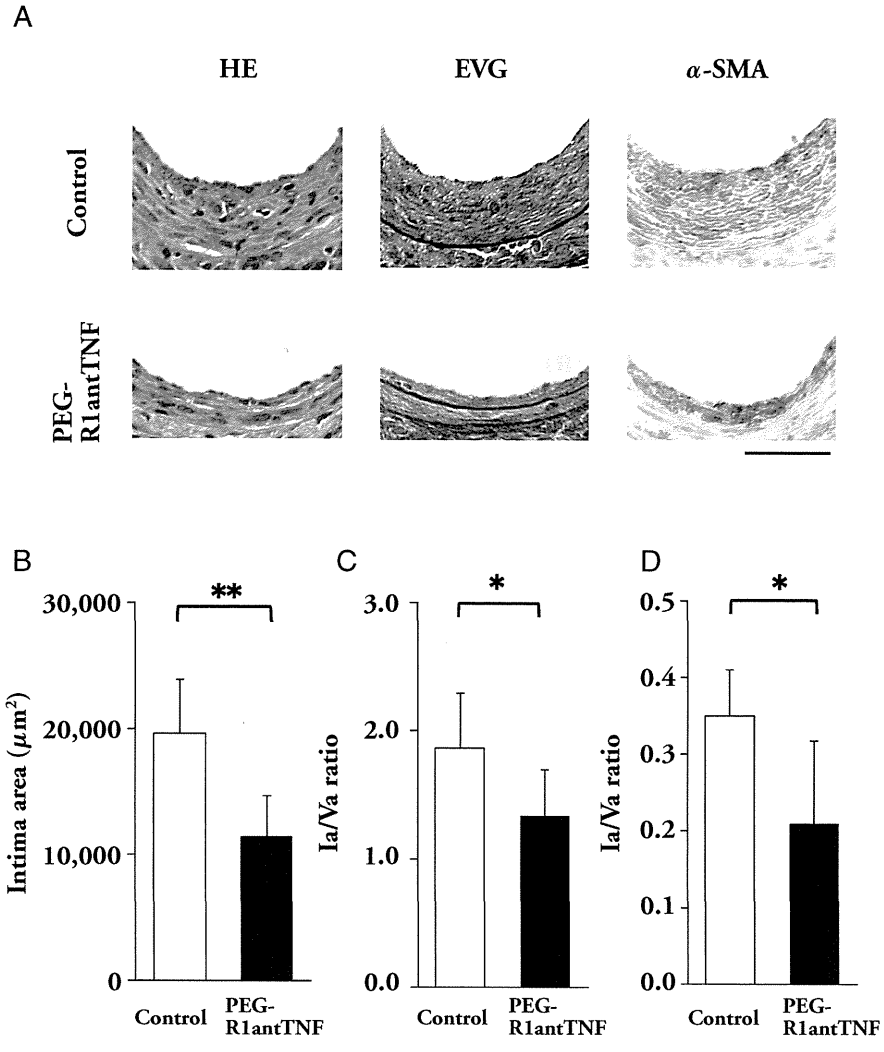

Fig. 3. PEG-R1antTNF significantly inhibited intimal hyperplasia in IL-1 Ra−/− arteries post-injury.

(A) Microscopic appearance of hematoxylin and eosin staining (left), elastica van Gieson staining (middle) and α-SMA staining (right) of femoral artery from control (upper panels) and PEG-R1antTNF (lower panels) groups 14 days post-injury. Scale bar = 50 μm. Bar graphs show intimal area (B), intima/media area ratio (C), and intima/vessel area ratio (D). Data are expressed as the mean ± SD ($n = 7$ for each). $^{*}p < 0.05$, $^{**}p < 0.01$.

The present study investigated the relationship between TNF signaling and arterial inflammation, revealing for the first time that TNFR1 signaling blocked by a TNFR1 antagonist might affect arterial inflammation and intimal hyperplasia in cuff-injured IL-1Ra-/- mice with severe inflammation around the artery, similar to Takayasu's disease[25]. Initially, we used wild-type C57BL/6J mice for the cuff injury model, but treatment induced little neointima formation in the control group. The lack of significant differences in intima area (3,222.9 ± 1,640.3 vs. 2,383.9 ± 618.7 μm^2; $p = 0.267$) and the intima area/media area ratio (0.278 ± 0.119 vs. 0.201 ± 0.060; $p = 0.179$) between the control and R1antTNF treatment group made it difficult to examine whether R1antTNF suppresses arterial inflammation and intimal hyperplasia. Previously, we reported that deficiency of IL-1Ra promotes intimal hyperplasia after femoral artery injury[18, 26]. We further determined that TNF-α deficiency suppresses aortitis in IL-1Ra-/- mice[27]. Thus,

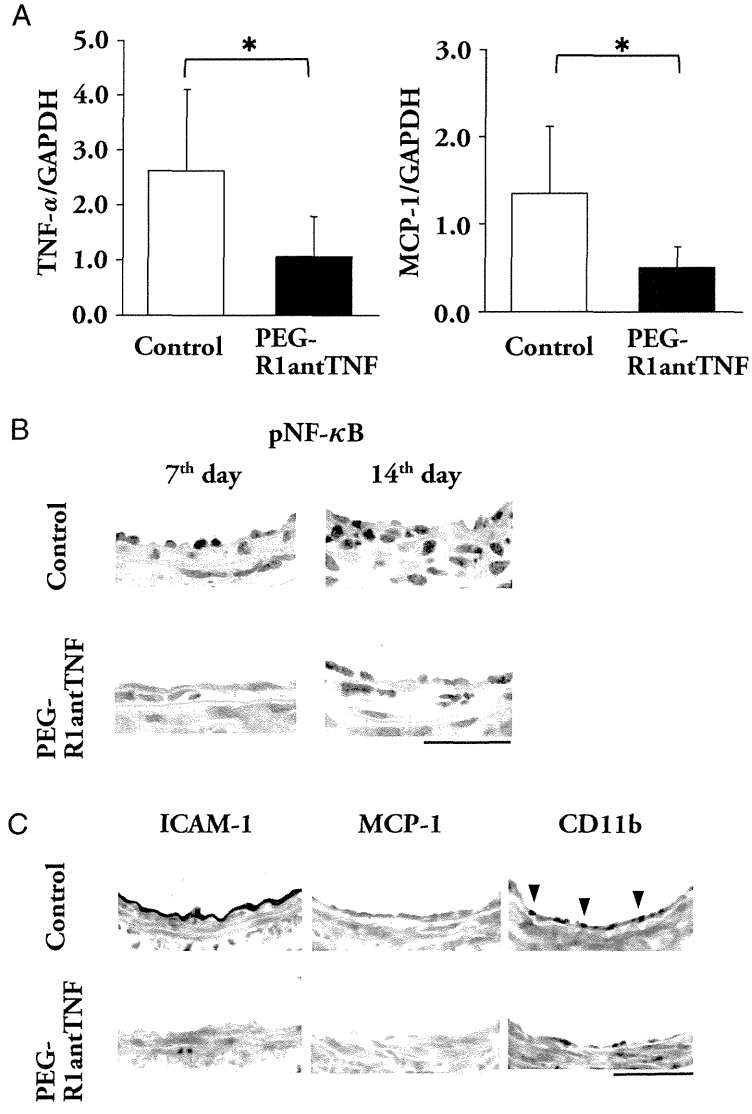

Fig. 4. PEG-R1antTNF suppressed TNF-α, adhesion molecule and chemokine, and activation of NF-κB.

(A) These graphs showed the amount of TNF-α (left; $n=7$) and MCP-1 (right; $n=5$) mRNA expression 5 days post-injury. Data are expressed as the mean ± SD. $^*p<0.05$. The result of immunostaining for pNF-κB-positive nucleus 7 and 14 days post-injury (B), expression of ICAM-1 (C; left), MCP-1 (C; middle), and CD11b (C; right) 7 days post-injury. Scale bar = 50 μm.

our findings suggest that TNF-α participates importantly in the development of arterial inflammation in IL-1Ra-/- mice. Consequently, we used IL-1Ra-/- mice in the present study because we believe that these mice were suitable for evaluating the effect of TNFR1 blocking therapy in active arterial inflammation induced by cuff injury.

The dose of PEG-R1antTNF in our study was determined according to a previous report showing PEG-R1antTNF was effective for the suppression of collagen-induced arthritis in mice[17]. The PEG-R1antTNF dose was not changed based on body weight, as infliximab and etanercept are also injected at the same dose independently of the body weight of the patients. Taken together, we think that the dose of PEG-R1ant TNF must be relevant in our study.

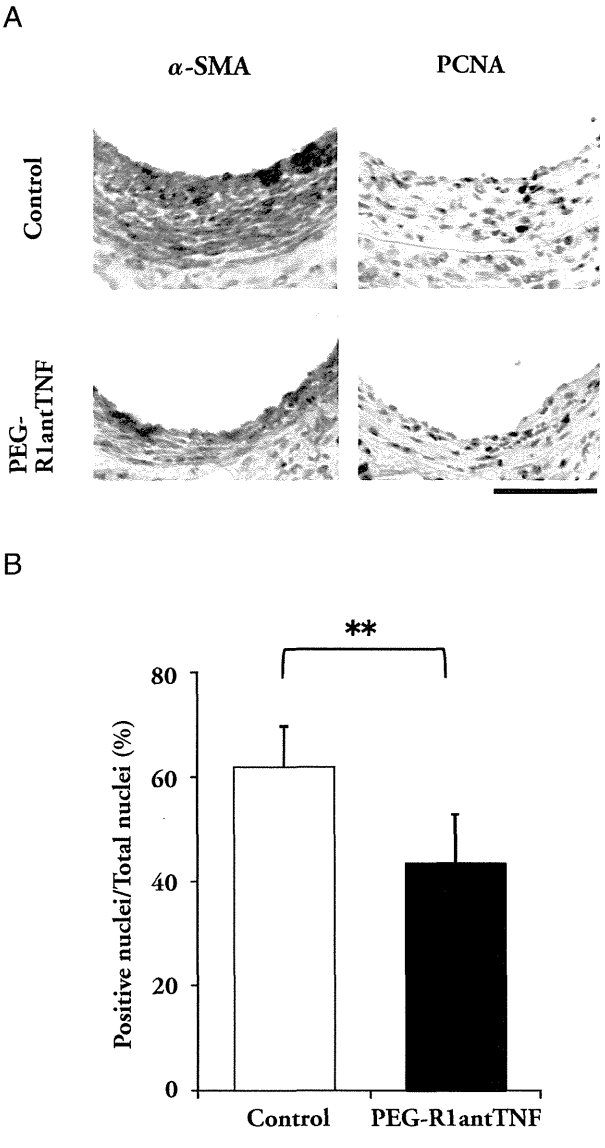

Fig. 5. PEG-R1antTNF inhibited cell proliferation in injured arteries.

(A) Representative photographs of α-SMA and PCNA staining of injured arteries 14 days post-injury. Scale bar = 50 μm. (B) Bar graph shows the number of PCNA-positive nuclei in the intima. Data are expressed as the mean ± SD ($n=6$). $^{**}p<0.01$.

A previous report showed that TNF-α activates IKK, induces the phosphorylation and ubiquitination of IκB, and activates NF-κB[28]. NF-κB is activated mainly via TNFR1 signaling, but only poorly via TNFR2-TNF receptor-associated factor 2 signaling[29]. NF-κB regulates macrophage migration and the expression of adhesion factor (ICAM-1)[30] and chemokine (MCP-1). NF-κB also regulates both the proliferation and migration of vascular SMCs[31-34]. Our results showed that blocking TNFR1 with R1antTNF decreased macrophage accumulation as well as ICAM-1 and MCP-1 expression by inhibiting NF-κB activation in endothelial cells and SMCs in the injured artery. Thus, TNFR1 signaling participates importantly in the development of intimal hyperplasia following arterial inflammation. Additionally, we show a relationship among inhibited intimal hyperplasia, suppressed NF-κB activation, adhesion factor and chemokine expression.

Zhang *et al.* examined the effect of TNF signaling through TNFR2 for intimal hyperplasia, demonstrating that TNFR2 signaling inhibits neointimal formation by decreasing adhered cells and endothelial cells apoptosis. They also showed that Etk/Bmx, a non-receptor tyrosine kinase, contributed to these results[9]. A previous study observed the anti-apoptotic effect of TNFR2, which specifically activates Etk/Bmx. TNFR2 also induces the activation, proliferation and migration of endothelial cells. Another study suggested that Etk/Bmx participates importantly in angiogenesis induced by TNF-α[35]. Thus, TNFR1-specific blocking therapy might aid the earlier regeneration of endothelial cells and inhibit intimal hyperplasia compared with TNF blocking therapy, which blocks both TNFR1 and TNFR2 signaling. Therefore, we examined whether R1antTNF treatment altered pEtk/Bmx expression in endothelial cells. Our results revealed no significant difference in pEtk/Bmx expression between groups. Similarly, our colleague, who used an index of GM-CSF production by TNF-α in PC60-R2 cells (a mouse-rat fusion hybridoma consisting of human TNFR2-transfected PC60 cells)[15], reported that R1antTNF did not affect bioactivity via TNFR2. These data suggest that R1antTNF does not stimulate endothelial cell regeneration in *in vitro* studies. In the future, we will examine whether R1antTNF treatment exerts an effect on Etk/Bmx activation via TNFR2 *in vivo*.

TNF-α forms a trimeric structure with various bioactivities[36]. We found that R1antTNF reacted with endogenous TNF-α to form a heterotrimer *in vitro* (unpublished data), possibly affecting the half-life and bioactivity of endogenous TNF-α *in vivo*. Thus, it remains undetermined whether the *in vivo* effects of R1antTNF might result only from inhibited TNFR1 signaling. Determining whether the trimer formation of R1antTNF and endogenous TNF-α might change the effect will require further study.

TNF blocking therapy improves vascular endothelial dysfunction and reduces cardiovascular events associated with inflammation in patients with rheu-